

Linear and Nonlinear Optical Properties of Cationic Bipyridyl Iridium (III) Complexes: Tunable and Photoswitchable?


Vincent Aubert,[†] Lucie Ordroneau,[†] Muriel Escadeillas,[†] J. A. Gareth Williams,[‡] Abdou Boucekkine,[†] Esther Coulaud,[†] Claudia Dragonetti,[§] Stefania Righetto,[§] Dominique Roberto,^{*,§} Renato Ugo,[§] Adriana Valore,[§] Anu Singh,^{||} Joseph Zyss,^{||} Isabelle Ledoux-Rak,^{||} Hubert Le Bozec,[†] and Véronique Guerschais^{*,†}

[†]UMR CNRS-Université de Rennes 1 6226, Université de Rennes 1, Campus de Beaulieu, 35042 Rennes Cedex, France

[‡]Department of Chemistry, University of Durham, South Road, Durham, DH1 3LE, United Kingdom

[§]Dip. CIMA "L. Malatesta" dell'Università di Milano, UDR-ISTM and ISTM-CNR, Via Venezian 21, 20133, Milano, Italy

^{||}Laboratoire de Photonique Quantique et Moléculaire UMR CNRS 8531, Institut d'Alembert, ENS Cachan, 61 Avenue du Président Wilson, 94235 Cachan, France

 Supporting Information

ABSTRACT: A series of cationic Ir(III) substituted bipyridyl ($N^{\wedge}N$ ($N^{\wedge}N$ -bpy) complexes incorporating electron-donor and -acceptor substituents, $[\text{Ir}(C^{\wedge}N\text{-ppy-R}')_2(N^{\wedge}N\text{-bpy-CH=CH-C}_6\text{H}_4\text{-R})][X]$ ($X^- = \text{PF}_6^-$ or $\text{C}_{12}\text{H}_25\text{SO}_3^-$), **2** (**a**, $R = \text{NEt}_2$ and $R' = \text{Me}$; **b**, $R = \text{O-Oct}$ and $R' = \text{Me}$; **c**, $R = \text{NO}_2$ and $R' = \text{C}_6\text{H}_{13}$; $C^{\wedge}N\text{-ppy} = \text{cyclometalated 2-phenylpyridine}$, $[\text{Ir}(C^{\wedge}N\text{-ppy-Me})_2(N^{\wedge}N\text{-bpy-CH=CH-thienyl-Me})][\text{PF}_6]$, **2d**, and the dithienylethene (DTE)-containing complex **2e** have been synthesized and characterized, and their absorption, luminescence, and quadratic nonlinear optical (NLO) properties are reported. Density functional theory (DFT) and time-dependent-DFT (TD-DFT) calculations on the complexes facilitate a detailed assignment of the excited states involved in the absorption and emission processes. All five complexes are luminescent in a rigid glass at 77 K, displaying vibronically structured spectra with long lifetimes (14–90 μs), attributed to triplet states localized on the styryl-appended bipyridines. The second-order NLO properties of **2a–d** and related complexes **1a–d** with 1,10-phenanthrolines have been investigated by both electric field induced second harmonic generation (EFISH) and harmonic light scattering (HLS) techniques. They are characterized by high negative EFISH $\mu\beta$ values which decrease when the ion pair strength between the cation and the counterion (PF_6^- , $\text{C}_{12}\text{H}_25\text{SO}_3^-$) increases. The EFISH response is mainly controlled by metal-to-ligand charge-transfer/ligand-to-ligand charge-transfer (MLCT/L'LCT) processes. A combination of HLS and EFISH techniques is used to evaluate both the dipolar and octupolar contributions to the total quadratic hyperpolarizability, demonstrating that the major contribution is controlled by the octupolar part. The incorporation of a photochromic DTE unit into the $N^{\wedge}N$ -bpy ligand (complex **2e**) allows the luminescence to be switched ON or OFF. The photocyclisation of the DTE unit can be triggered by using either UV (365 nm) or visible light (430 nm), leading to an efficient quenching of the ligand-based 77 K luminescence, which can be restored upon irradiation of the closed form at 715 nm. In contrast, no significant modification of the EFISH $\mu\beta$ value is observed upon photocyclization, suggesting that the quadratic NLO response is dominated by the MLCT/L'LCT processes, rather than by the intraligand excited states localized on the substituted bipyridine ligand.

INTRODUCTION

In the area of new molecular materials for photonic and optoelectronic applications, the impact of coordination and organometallic complexes of transition metals has increased dramatically during the last two decades.¹ For instance, there has been growing interest in luminescent iridium(III) complexes due to their high quantum efficiency and color tunability. Various cyclometalated Ir complexes have been reported, which can be classified into two main groups: neutral complexes, such as $\text{Ir}(C^{\wedge}N\text{-ppy})_3^{2a-m}$ or $\text{Ir}(C^{\wedge}N\text{-ppy})_2(L^{\wedge}X)^{3,4a-4j}$ (where $C^{\wedge}N\text{-ppy}$ represents cyclometalated 2-phenylpyridine ligands and $L^{\wedge}X$ represents a monoanionic ancillary ligand), and cationic complexes such as $[\text{Ir}(CN\text{-ppy})_2(N^{\wedge}N)]^+$, featuring diimine ligands.^{5,6a,6b,7,8} It is well-known that the nature of the coordinated $C^{\wedge}N$ or $N^{\wedge}N$ ligand can strongly affect the photophysical

and electrochemical properties of iridium(III) complexes. The metal-to-ligand and intraligand charge-transfer transitions (MLCT and ILCT) which govern the optical properties in these cyclometalated complexes are readily modulated by incorporating electron-withdrawing/donating groups on the diimine ligand. For example, electronic tuning has recently been investigated in a series of cationic cyclometalated iridium complexes containing substituted 1,10-phenanthrolines⁹ **1a–d** (Figure 1). This work has shown that the nature and the number of substituents on the 1,10-phenanthroline (phen) ligand can significantly affect the quantum yields and lifetimes of the corresponding complexes by influencing the relative magnitudes of the radiative decay processes, even

Received: February 10, 2011

Published: April 25, 2011

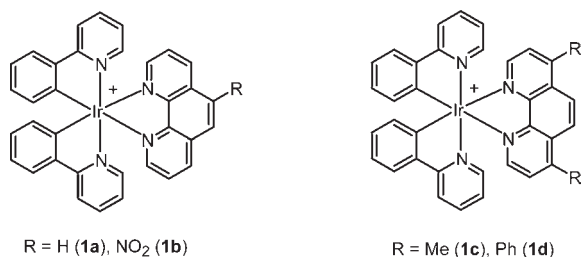


Figure 1. Cationic bis-cyclometalated Ir(III) complexes incorporating substituted phenanthroline ligands.

though the absorption and the emission energies are only modestly affected.

Some of us have been involved in the design of 4,4'-disubstituted-[2,2']-bipyridines not only as fluorophores in their own right but also as precursors to dipolar and octupolar metal complexes. From the wide range of 4,4'- π -conjugated bipyridyl ligands prepared, such as 4,4'-bis(donor-styryl)-[2,2']-bipyridines, we have previously shown how simple modification of the π -linker and the donor end groups enables the generation of tunable chromophores and fluorophores.^{10,11} Continuing our effort to probe the structural factors that could improve the optical and nonlinear optical (NLO) properties of π -conjugated bipyridyl metal complexes, we describe in this article the chemistry and the photophysical studies of a new series of iridium(III) complexes [Ir(C[^]N-ppy-Me)₂(N[^]N-bpy-CH=CH-Ar-R)]⁺[X⁻] (X⁻ = PF₆⁻ or C₁₂H₂₅SO₃⁻), 2a–d, which incorporate extended Ar-vinyl π systems on the bipyridine ligand (Ar = 1,4-substituted benzene ring or 2,5-substituted thienyl ring). The systematic variation of R was anticipated to allow the modulation of their linear and NLO properties (Figure 2).

Our previous observation that complexes, such as [Ir(C[^]N-ppy)₂(5-R-phen)]⁺[X⁻] (1a, R = H; 1b, R = NO₂) and [Ir(C[^]N-ppy)₂(4-R,7-R-1,10-phen)]⁺[X⁻] (1c, R = Me, 1d, R = Ph) are characterized by a large second-order NLO response¹² [measured as $\mu\beta_{1,907}$ by the electric field induced second harmonic generation (EFISH) technique working in CH₂Cl₂ with a 1.907 μ m wavelength] prompted us to extend our NLO study to these new cationic bipyridine cyclometalated Ir(III) complexes 2a–d functionalized with donor or acceptor substituents. In order to understand more clearly their second-order NLO properties, both families of complexes are also analyzed by the complementary harmonic light scattering (HLS) technique. A combination of HLS and EFISH data are then used to evaluate both the dipolar and octupolar contributions to the quadratic hyperpolarizability of 1b and 2c as representative cationic Ir(III) complexes.

Finally, in the context of the modulation of optical and NLO properties of polypyridyl metal complexes, we have previously developed a new type of photochromic 4,4'-bis(ethenyl)-2,2'-bipyridine ligand functionalized by a dimethylaminophenyl-dithienylethene (DTE) group (Le) and the corresponding (bipyridyl)zinc(II) complex.¹³ DTE derivatives are well-known to undergo reversible interconversion between a nonconjugated open form and a π -conjugated closed form when irradiated in the UV and visible spectral ranges, respectively.¹⁴ We have exploited this property to design the first example of metal-containing photochromic ligands allowing an efficient switching of the quadratic NLO properties.^{13a} In the present work, we have sought to combine the photochromic DTE-based bipyridine ligand Le with a luminescent bis-cyclometalated Ir(III) center in order to study

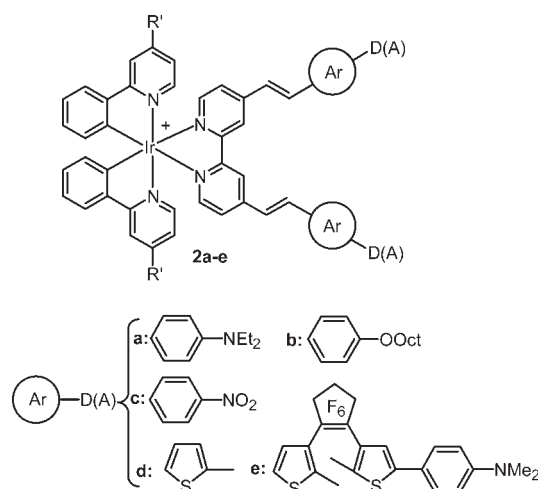


Figure 2. Cyclometalated cationic bipyridine Ir(III) complexes.

the photoregulation of the emission and the NLO properties of the resulting system. The use of a single photochromic ligand for photocontrol of both NLO and luminescence properties has not previously been investigated.¹⁵

RESULTS AND DISCUSSION

Synthesis and Characterization of the Bipyridine Ligands and their Ir Complexes. The R-styryl-appended bipyridine ligands bpy-C₆H₄-CH=CH-R, La–c (a, R = NEt₂; b, R = O-Oct; c, R = NO₂) were synthesized according to previous published procedures.^{10a–c} The thienyl derivative Ld is obtained as a yellow powder in 67% yield by treatment of 4,4'-dimethylbipyridine with 5-methylthiophene-2-carbaldehyde in the presence of ^tBuOK in THF. The preparation of the DTE-based bipyridine ligand Le (o: open form) has been described previously.^{13a}

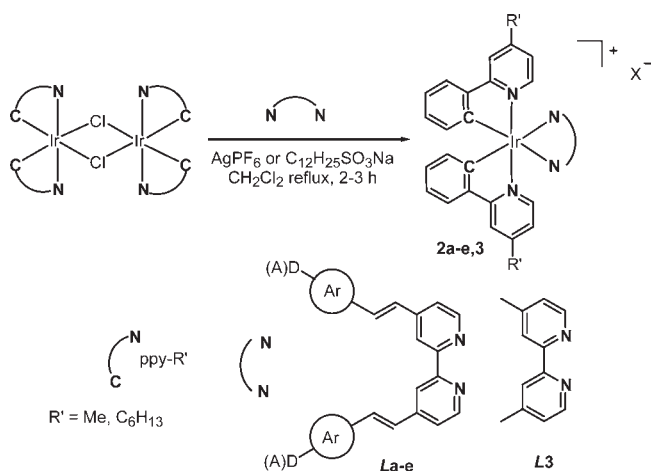
The cationic Ir(III) complexes Ir(C[^]N-ppy-R')₂(N[^]N-bpy-CH=CH-Ar-R)]PF₆ (R' = Me, C₆H₁₃) 2a–e were readily synthesized upon treatment of the corresponding μ -chloro dimer [Ir(N[^]C-ppy-R')₂(μ -Cl)]₂ with the appropriate bipyridyl ligand L in the presence of AgPF₆ (Scheme 1). A methyl group (R = Me) was incorporated in the four position of the pyridine moiety of the ppy ligand in order to facilitate NMR studies, while R = C₆H₁₃ in the nitro complex 2c to improve its solubility. The ppy-Me ligand was prepared by standard procedures¹⁶ and converted to ppy-C₆H₁₃ by treatment with LDA, followed by addition of C₅H₁₁I. All complexes are thermally stable and were isolated as orange-red solids in good yield; they have been fully characterized by ¹H and ¹³C NMR spectroscopy as EE isomers. However, in CH₂Cl₂ solution, complexes 2a–d undergo an isomerization process of the C=C double bond under UV irradiation, ¹H NMR spectroscopy indicating partial conversion to the Z/Z and/or E/Z isomers. This phenomenon has been observed previously for related neutral bis- and tris-cyclometalated Ir complexes carrying styryl substituents in the ligands.¹⁶

Although the nitro ligand Lc is essentially insoluble in common organic solvents, its complex 2c, incorporating ppy-C₆H₁₃ coligands, is partially soluble in CH₂Cl₂. All the complexes were isolated as their hexafluorophosphate salts. For the purpose of investigating the influence of the counterion on the NLO properties, the dodecanesulfonate salts of 2a and 2c were also

prepared. They were isolated by using $C_{12}H_{25}SO_3Na$ in place of $AgPF_6$ in the reaction of the μ -chloro dimer with the ligands L .¹²

Ground-State UV–Vis Absorption Properties. The UV–vis spectra of the four complexes **2a–d** in solution at room temperature are displayed in Figure 3, with the main absorption maxima and extinction coefficients summarized in Table 1. All four complexes show very intense bands at $\lambda > 300$ nm ($\epsilon > 30\,000\text{ M}^{-1}\text{cm}^{-1}$), decreasing in energy in the order $NO_2 > O\text{-Oct} > \text{thiophene} > N\text{Et}_2$. While absorption bands due to MLCT transitions are typically anticipated around 400 nm for $[Ir(C^{\wedge}N)_2(N^{\wedge}N)]^+$ complexes,^{5–7,17a} the bands in the region 300–500 nm for **2a–d** are around an order of magnitude more

Scheme 1. Synthesis of Cyclometalated Cationic Bipyridine Ir(III) Complexes^a



^a The substituents in the bipyridines **a–e** are as shown in Figure 2.

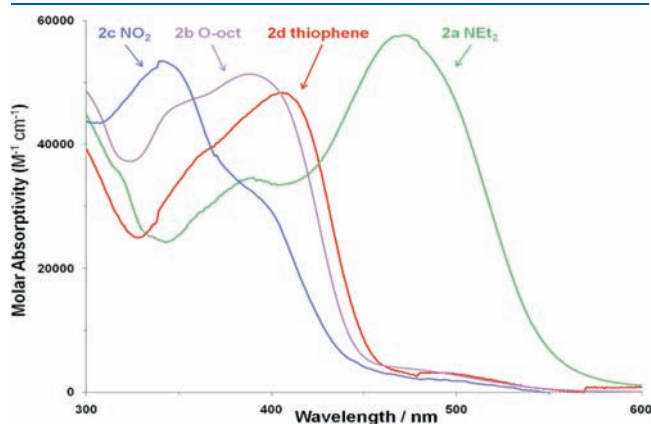


Figure 3. UV–vis spectra of complexes **2a–d** in CH_2Cl_2 .

Table 1. Electronic Absorption Spectral (298 K) and Luminescence Data for Ir Complexes **2a–d** and **3** (77 K)

complex	$\lambda_{\text{abs}}/\text{nm}$ ($\epsilon/\text{M}^{-1}\text{cm}^{-1}$) ^a	$\lambda_{\text{em}}/\text{nm}$ ^b	$\tau/\mu\text{s}$
2a	390(35 500), 473(59 000)	656, 724, 798	90
2b	360sh(47 600), 388(51 400)	608, 670, 736	38
2c	338(52 500), 390(32 200)	618, 683, 744	14
2d	360(39 200), 406(48 400)	658, 732, 809	34
3	300sh (21 000), 345sh (12 000), 380 (6900), 420 (4100), 470 (1000)	506	4.8

^a At 298 K in CH_2Cl_2 . ^b At 77 K in ether/isopentane/ethanol (2:2:1, v/v).

intense than expected for such transitions. They are attributed to intraligand (IL) transitions within the styryl-substituted bipyridine ligands, which are red shifted compared to those of the free ligands,^{10c} due to a lowering of the lowest unoccupied molecular orbital (LUMO) energy level upon coordination of the pyridine rings. The weaker MLCT and ligand-to-ligand charge-transfer (L/LCT) transitions are likely to be obscured by these bands. However, there is evidence of a weaker band or bands tailing further into the visible (up to 560 nm) for **2b–d**, which may be due to excitation to the triplet CT states, as typically observed in related bis-cyclometalated iridium(III) complexes.¹⁷

The absorption spectrum of the diethylamino complex **2a** displays a particularly low-energy absorption band (473 nm), which is anticipated to arise from an IL transition on the bpy-styryl- $N\text{Et}_2$ ligand, but featuring a high degree of ILCT character and more extensive participation of the pendent amine. The time-dependent-DFT (TD-DFT) calculations discussed in the next section provide further insight into the nature of the transitions in the four complexes, broadly supporting these qualitative interpretations.

Computational Studies. DFT calculations were carried out on three complexes (**2a**, **2c**, **2d**) using PBE0 and the basis set described in the Experimental Section to get insight into the electronic structures of the complexes. Geometry optimizations were performed: The calculated metric parameters (Table 2) for **2a** [Ir– N_{bpy} (2.146 Å), Ir–C (1.998 Å), $C_{\text{bpy}}\text{–}C_{\text{bpy}}$ (1.483 Å), and C=C (1.363 Å)] and **2c** [Ir– N_{bpy} (2.145 Å), Ir–C (1.999 Å), $C_{\text{bpy}}\text{–}C_{\text{bpy}}$ (1.482 Å), and C=C (1.354 Å)] compare favorably to the crystallographically determined values reported in the literature for related systems.¹⁸ The R-styryl groups are coplanar with the two pyridyl rings, as clearly exemplified in the case of complex **2c** shown in Figure 4. This planarity is a critical parameter for efficient conjugation and charge transfer during excitations.

The TD-DFT calculations demonstrate that the identity of the vinyl-bipyridine substituent alters the nature of the frontier orbitals (Figure 5). For complex **2a**, the highest occupied molecular orbitals (HOMO) and HOMO–1, which are quasidegenerate, and the LUMO and LUMO+1 are almost exclusively localized on the aminostyryl-bipyridine ligand; the calculated metal (5d-Ir) contribution to HOMO and HOMO–1 orbitals is only 1–2%. It is noteworthy that the HOMO(HOMO–1), LUMO, and LUMO+1 orbitals are within the same plane: The HOMOs are predominantly localized on the diethylaminophenyl fragment of the ligand, while the LUMO and LUMO+1 correspond to the π^* orbitals of the bipyridine ligand, the main acceptor (Figure 5). The electronic absorption spectrum calculated by TD-DFT (Figure 6a) qualitatively matches that observed experimentally (Figure 3), albeit with an underestimation of the energies of the bands. The low-energy absorption band is composed of a combination of two excitations from HOMO to LUMO and HOMO–2 to LUMO, which could be designated as

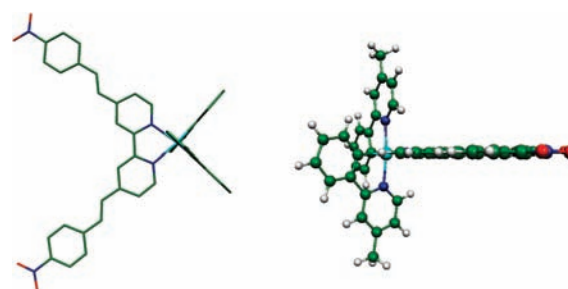
Table 2. Distances (Å) and Angles (°) of Optimized Structures of Ir Complexes

complex	distances (Å)			angles (°)		
	Ir–N	Ir–C	C _{bpy} –C _{bpy}	C=C	N–Ir–N	N–Ir–C
2a	2.146	1.998	1.483	1.363	76.0	97.5
2c	2.145	1.999	1.482	1.354	76.0	97.5
2d	2.145	1.998	1.483	1.361	76.0	97.4
3	2.130	2.016	1.460	–	76.7	97.3

ILCT and LL'CT/MLCT (33% metal contribution) transitions, respectively, based on the corresponding molecular orbitals (Table 3). The presence of the two cyclometalating carbon ligands has a significant influence leading to a comparable energy for HOMO-2 and HOMO orbitals. However, the poor overlap of orbitals in this transition leads to a lower oscillator strength, such that it will be the ILCT component that is likely to dominate the lower-energy part of the absorption spectrum. The higher-energy transition appears to be dominated by excitation of HOMO (HOMO-1) to LUMO+1, which can be assigned as a $\pi-\pi^*$ transition within the π -conjugated bipyridine ligand. This transition differs from the lower energy one in that it has a lower degree of CT character.

The presence of an electron-withdrawing group, such as NO₂ in **2c**, leads to frontier MOs which are different from those calculated for **2a** (Figure 6). The HOMO is of an antibonding combination of Ir(33%) and ppy(π) orbitals. The LUMO is very similar to that of **2a**, entirely localized on the vinyl-bipyridine fragments. A significant participation of the cyclometalating rings in the three first HOMOs is observed. The computed absorption spectrum of **2c** (Figure 6b) compares well with the experimental one (Figure 3). In particular, the blue shift of the nitro complex **2c** compared to the amino complex **2a** is reproduced. The displacement of the highest occupied orbitals from being localized on the styryl pendant in **2a** to the metal/ppy ligand in **2c** is intuitively reasonable given the electron-rich nature of the amine substituent in the former and the strongly electron-withdrawing character of the nitro group in the latter. The TD-DFT shows that the higher-energy band essentially corresponds to HOMO-6 to LUMO and HOMO-7 to LUMO, respectively (Table 3). The metal character is high in both HOMO-6 and HOMO-7. Moving to lower energy, the L'LCT contribution increases: The band into the visible is due to excitation from HOMO-3 and HOMO-1 to LUMO, where HOMO-3 is exclusively composed of metal (22%) and the phenyl orbitals (Figure 5). This allows the assignment of the visible band as mixed MLCT/L'LCT character.

Introducing an electron-donating (NEt₂) or electron-withdrawing (NO₂) group on the styrylbipyridine ligand leads to almost identical HOMO–LUMO gaps (**2a**: 2.69 eV, **2c**: 2.77 eV), although the calculated energy levels of the frontier orbitals are different (HOMO: –6.99 eV (**2a**), –8.19, (**2c**); LUMO –4.30 eV (**2a**), 5.42 (**2c**)) (see Supporting Information). It is noteworthy that there is a significant (1.2 eV) stabilization of the HOMO level of **2c** (–8.19 eV), compared to that of the amino complex **2a** (–6.99 eV), while the LUMO level decreases by 1.1 eV on going from **2a** to **2c**. In addition, we demonstrate that the presence of the π -conjugated styryl group leads to a net decrease of the HOMO–LUMO gap compared to that of the methyl derivative **3** (3.06 V).

**Figure 4.** Optimized geometry for complex **2c**.

The calculated spectrum of the thienyl complex **2d** displays two intense bands at 374 and 456 nm, due to a mixture of IL and MLCT transitions. The three HOMO and LUMO obtained from the calculations are shown in the Supporting Information. The HOMO–LUMO gap (3.01 V) is slightly larger than those of **2a** and **2c**.

Emission Spectroscopy. None of the complexes **2a–d** display detectable luminescence in solution at room temperature when excited in the UV or visible bands, in contrast to the uncoordinated ligands **La,b** whose room temperature fluorescence has been reported previously.^{10c} We have noted a similar phenomenon of lack of emission—or only weak emission—for related neutral cyclometalated Ir and Pt complexes carrying styryl substituents in the ligands, [Ir(C^N-ppy-CH=CH-C₆H₄-R)₂-(acac)]^{16b} (acac = acetylacetonate) and [Pt(C^N-ppy-CH=CH-C₆H₄-R)(acac)]¹⁹ (R = H, NO₂, OMe, NEt₂). The quenching of the emission in these systems has been interpreted in terms of competitive deactivation of the excited state through the *E–Z* isomerization process. Such an argument is again supported in the present instance by the ¹H NMR observations described earlier, which show the formation of the *Z* isomer upon irradiation.

At 77 K (EPA), all the complexes emit (Figure 7 and Table 1), displaying highly structured luminescence spectra with vibronic progressions of 1500 cm⁻¹, typical of aromatic and/or C=C bond vibrations. Evidently, in a rigid matrix at 77 K, the *E–Z* isomerization process cannot occur, allowing emission to be observed. The emission maxima lie in the order O-Oct < nitro < amino < thiophene, which is different from the order of energies of the absorption bands. The long lifetimes (tens of μ s), low-energy, and highly structured spectra are indicative of emission from a triplet state predominantly localized on the styryl-appended ligands, rather than from the MLCT state. For example, for the ³MLCT emission of complex **3**, incorporating 4,4'-methyl-2,2'-bipyridine as the N^N ligand, the luminescence lifetime at 77 K is 4.83 μ s; $\lambda_{em}^{max} = 506$ nm. It is notable that the shortest lifetime among the four complexes is that of the nitro complex **2c**, while the longest is that of the amino complex **2a** ($\tau = 14$ and 90 μ s respectively), which would be consistent with the TD-DFT results that indicate a more significant MLCT contribution to the lowest excited states of the former, compared to more pure ILCT character in the latter. The participation of the metal is required in order to promote the formally forbidden triplet radiative decay. Some caution must be applied here, however, since the TD-DFT results apply to the singlet states, while the differing order of energies in emission compared to absorption suggests a different orbital parentage of the emissive triplet states compared to the singlets.

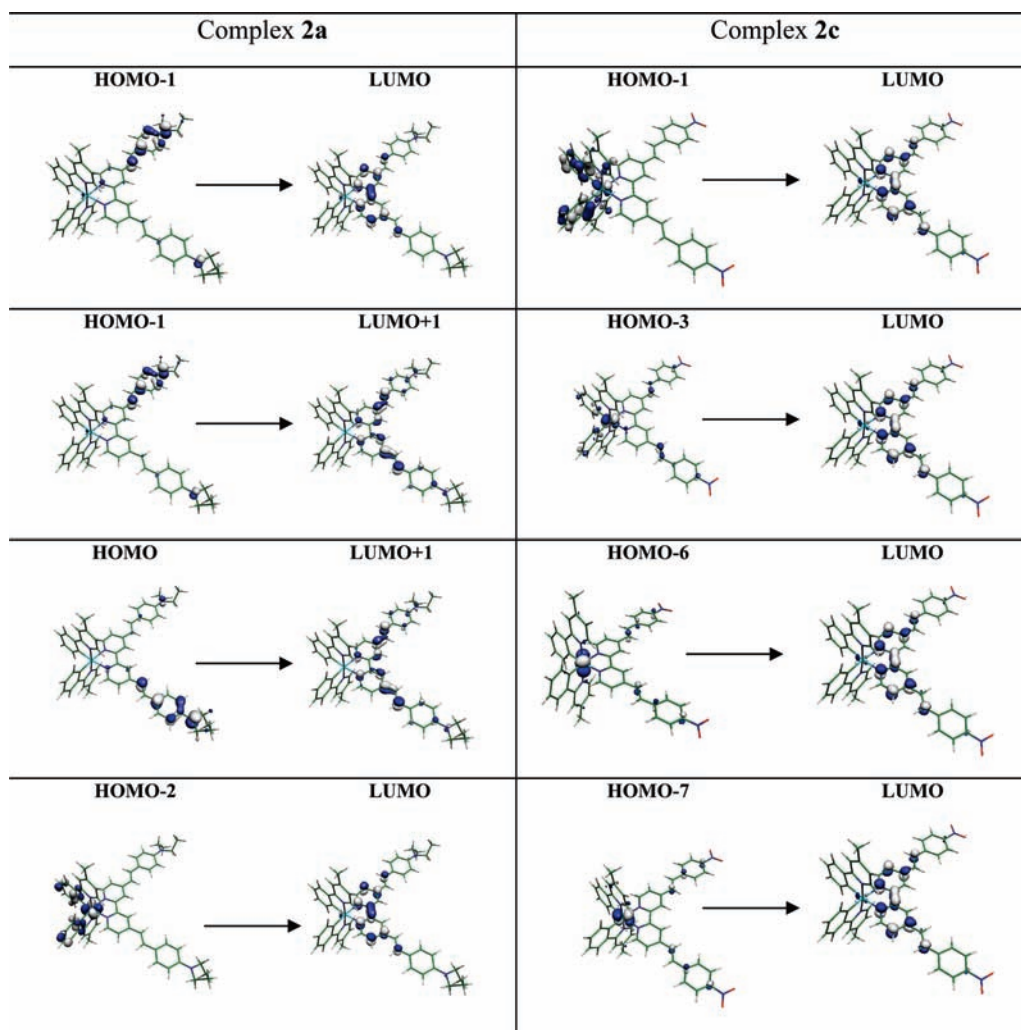


Figure 5. Molecular orbitals of selected transitions involved in the singlet excited states of complexes 2a (left) and 2c (right) calculated by TD-DFT.

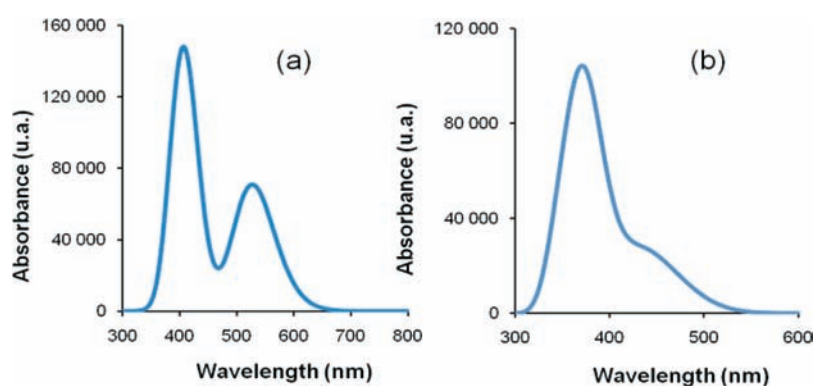


Figure 6. Calculated electronic absorption spectra of complexes 2a (a) and 2c (b).

Quadratic NLO Studies. The second-order NLO responses of the new complexes **2a–d** [$X^- = \text{PF}_6^-$], **2a,c** [$X^- = \text{C}_{12}\text{H}_{25}\text{SO}_3^-$], and **3** [$X^- = \text{PF}_6^-$] were determined by the EFISH technique, working with an incident wavelength of $1.907 \mu\text{m}$ in CH_2Cl_2 solution (concentration = 10^{-3} M), a low-polarity solvent which allows the extension of the use of this technique to ionic compounds by virtue of the significant ion-pairing.^{12b,20} The

values of EFISH $\mu\beta_{1.907}$ are reported in Table 4, along with those previously reported¹² for **1a** [$X^- = \text{PF}_6^-$], **1b** [$X^- = \text{PF}_6^-$, $X^- = \text{C}_{12}\text{H}_{25}\text{SO}_3^-$], and **1c** and **1d** [$X^- = \text{PF}_6^-$]. As evidenced in Table 4, the EFISH $\mu\beta_{1.907}$ of **3** is similar to that of **1c**, showing that the use of simply substituted bipyridines in place of phenanthrolines does not affect the second-order NLO response of $[\text{Ir}(\text{C}^{\wedge}\text{N})_2(\text{N}^{\wedge}\text{N})]^+$ complexes nor does the introduction of

Table 3. Energies, Corresponding Wavelengths, And Oscillator Strengths for the Lowest-Lying Excited States of Complexes **2a** and **2c** as Determined by TD-DFT, Together with Their Main Molecular Orbital Compositions and Assignments

λ (nm)	E (eV)	f	transition (contribution)	assignment
Complex 2a				
539	2.30	0.407	HOMO→LUMO (70%)	ILCT
			HOMO-2→LUMO (22%)	MLCT/L/LCT
524	2.36	0.145	HOMO-2→LUMO (76%)	MLCT/L/LCT
			HOMO→LUMO (21%)	ILCT
518	2.39	0.458	HOMO-1 → LUMO (88%)	ILCT
417	2.97	0.861	HOMO-1→ LUMO+1 (87%)	IL
407	3.05	0.781	HOMO → LUMO+1 (76%)	IL
Complex 2c				
469	2.64	0.071	HOMO-1 → LUMO (95%)	MLCT/L/LCT
434	2.86	0.264	HOMO-3 → LUMO (91%)	MLCT/L/LCT
373	3.32	0.772	HOMO-6 → LUMO (70%)	MLCT
350	3.54	0.350	HOMO-7 → LUMO (59%)	MLCT

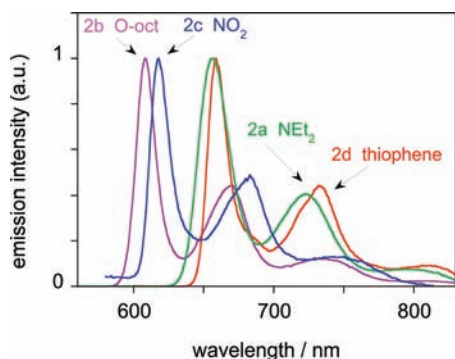


Figure 7. Normalized emission spectra of complexes **2a–d** at 77 K in diethyl ether/isopentane/ethanol (2:2:1 v/v), upon excitation into the lowest-energy absorption band.

the methyl substituent in ppy ligands. An increase of the absolute value of EFISH $\mu\beta_{1,907}$ is observed by increasing the π delocalization of the 2,2'-bipyridine with styryl substituents, reaching values even higher than that previously reported¹² for the Ir(III) complex with 5-nitro-1,10-phenanthroline **1b**. As for the latter complex, the absolute values of EFISH $\mu\beta_{1,907}$ of **2a–d** are found to increase upon dilution from 10^{-3} to 10^{-4} M, due to an increase of the percentage of free ions from ca. 60 to 80%, as confirmed by ¹H and ¹⁹F pulsed gradient spin-echo (PGSE) NMR spectroscopy.²¹ Moreover, working at the same concentration of 10^{-3} M in CH₂Cl₂, the value recorded is lowered upon substitution of PF₆⁻ by C₁₂H₂₅SO₃⁻, as expected for an increase of the ion-pair strength for sulfonate as the counterion compared to hexafluorophosphate^{12b} (compare **2a**[PF₆⁻] with **2a**[C₁₂H₂₅SO₃⁻] and **2c**[PF₆⁻] with **2c**[C₁₂H₂₅SO₃⁻] in Table 4).

The data presented in Table 4 show that the nature of the substituents on the π -delocalized 2,2'-bipyridines of **2a–d** does not affect significantly the global $\mu\beta_{1,907}$ values. In the related Ir(III) complexes with 5-R-1,10-phenanthrolines **1a–d**, sum over states (SOS)-TD-DFT investigations showed that when R is a strong electron-withdrawing group, like NO₂, the EFISH

Table 4. EFISH $\mu\beta_{1,907}$ and HLS $\beta_{1,907}$ Values of All Investigated Complexes in CH₂Cl₂

complex	X ⁻	EFISH $\mu\beta^a$ (10^{-48} esu)	$\langle\beta_{\text{HLS}}\rangle^a$ (10^{-30} esu)
1a	PF ₆ ⁻	-1270 ^b	460
1b	PF ₆ ⁻	-2230 ^b	375 ^c
1b	C ₁₂ H ₂₅ SO ₃ ⁻	-1430 ^b	410 ^c
1c	PF ₆ ⁻	-1454 ^b	377
1d	PF ₆ ⁻	-1997 ^b	460
2a	PF ₆ ⁻	-2770 ^d	540
2a	C ₁₂ H ₂₅ SO ₃ ⁻	-1015	420
2b	PF ₆ ⁻	-2430 ^d	468
2c	PF ₆ ⁻	-2770 ^d	432 ^c
2c	C ₁₂ H ₂₅ SO ₃ ⁻	-1250	393 ^c
2d	PF ₆ ⁻	-2386 ^d	550
3	PF ₆ ⁻	-1420	520

^a Values obtained working at a concentration of 10^{-3} M; estimated uncertainty in EFISH and HLS measurements is $\pm 10\%$. ^b From ref 12b. ^c In deuterated DMF, the $\langle\beta_{\text{HLS}}\rangle$ value is 340, 402, 432, and 382 $\times 10^{-30}$ esu for [**1b**][PF₆], [**1b**][C₁₂H₂₅SO₃], [**2c**][PF₆] and [**2c**][C₁₂H₂₅SO₃], respectively. ^d Working at 10^{-4} M in CH₂Cl₂, the EFISH $\mu\beta_{1,907}$ values increase to -3600, -3450, -4660, and -2998 $\times 10^{-48}$ esu for [**2a**][PF₆], [**2b**][PF₆], [**2c**][PF₆], and [**2d**][PF₆].

quadratic hyperpolarizability is exclusively the sum of negative contributions, arising mainly from L/LCT/MLCT excitations involving the π^* phenanthroline orbitals as acceptors, whereas when R is an electron-donor group, like NMe₂, there are counteracting positive (ILCT) and negative (L/LCT/MLCT) contributions to the EFISH quadratic hyperpolarizability, with the latter controlling the negative sign of the converged final value.¹² A similar behavior is expected in the case of the Ir(III) complexes with π delocalized 2,2'-bipyridines. Besides, the dipole moment of the strong ion-pairs **1b**[C₁₂H₂₅SO₃⁻] (18 D) and **2c**[C₁₂H₂₅SO₃⁻] (12 D) could be determined experimentally by the Guggenheim method,²² showing that the absolute value of EFISH $\beta_{1,907}$ is higher for the complex with the π -delocalized 2,2'-bipyridine bearing two strong electron-withdrawing NO₂ groups (Table 5), in agreement with an EFISH response mainly controlled by MLCT/L/LCT processes from the cyclometalated phenylpyridine Ir(III) moiety, acting as donor system, to the π^* orbitals of the bipyridine, acting as an acceptor system.

Remarkably, all investigated cyclometalated Ir(III) complexes with substituted 1,10-phenanthrolines and 2,2'-bipyridines are characterized by a large value of $\langle\beta_{\text{HLS},1,907}\rangle$ ($375\text{--}550 \times 10^{-30}$ esu), in CH₂Cl₂ solution (Table 4). This value does not change significantly with the nature of the counterion (PF₆⁻ or C₁₂H₂₅SO₃⁻), suggesting that the HLS second-order NLO response of these cationic cyclometalated Ir(III) complexes is not affected by the strength of the ion pairs. Further evidence in support of this conclusion comes from the observation that similar $\langle\beta_{\text{HLS},1,907}\rangle$ values were obtained in deuterated DMF,²³ a solvent which, contrary to CH₂Cl₂, cleaves ion pairs (Table 4).

In order to evaluate the dipolar ($J = 1$) and octupolar ($J = 3$) contributions to the total quadratic hyperpolarizability (eq 1) of both families of cationic cyclometalated Ir(III) complexes, we can use a combination of the EFISH and HLS techniques (Table 5).²⁴ In fact, for a molecule with a C_{2v} symmetry the dipolar contribution $\|J^{J=1}\|$ can be calculated from β_{EFISH} with eq 2. When the value of $\langle\beta_{\text{HLS}}\rangle$ is known, the octupolar

Table 5. Dipole Moments (μ), β_{EFISH} , $\langle\beta_{\text{HLS}}\rangle$, and Dipolar and Octupolar Contributions of the Quadratic Hyperpolarizability of [1b][C₁₂H₂₅SO₃] and [2c][C₁₂H₂₅SO₃]

complex	μ^a (D)	$\langle\beta_{\text{EFISH}}\rangle^b$ (10^{-30} esu)	$\langle\beta_{\text{HLS}}\rangle^b$ (10^{-30} esu)	$\ \beta^{J=1}\ $ (10^{-30} esu)	$\ \beta^{J=3}\ ^c$ (10^{-30} esu)	ε^d (10^{-30} esu)
1b[C ₁₂ H ₂₅ SO ₃]	18	-79	410	-61	1325	916
2c[C ₁₂ H ₂₅ SO ₃]	12	-104	393	-81	1267	876

^aIn CHCl₃; the error on μ is ± 1 D. ^bIn CH₂Cl₂; the error of EFISH and HLS measurements is $\pm 10\%$. ^cThe total quadratic hyperpolarizability (from eq 1) is 1326 and 1269×10^{-30} esu for [1b][C₁₂H₂₅SO₃] and [2c][C₁₂H₂₅SO₃], respectively. ^d ε is the difference between the total quadratic hyperpolarizability (from eq 1) and $\langle\beta_{\text{HLS}}\rangle$.

contribution $\|\beta^{J=3}\|$ can then be obtained by application of eq 3.²⁵

$$\|\bar{\beta}\|^2 = \|\bar{\beta}^{J=1}\|^2 + \|\bar{\beta}^{J=3}\|^2 \quad (1)$$

$$\|\beta^{J=1}\| = \sqrt{\frac{3}{5}}\beta_{\text{EFISH}} \quad (2)$$

$$\langle\beta_{\text{HLS}}^2\rangle = \langle|\beta_{\text{XXX}}|^2\rangle + \langle|\beta_{\text{ZXX}}|^2\rangle = \frac{2}{9}\|\bar{\beta}^{J=1}\|^2 + \frac{2}{21}\|\bar{\beta}^{J=3}\|^2 \quad (3)$$

As shown in Table 5, these high values of $\langle\beta_{\text{HLS}}\rangle$ are due to a high-octupolar $\|\beta^{J=3}\|$ component, the dipolar component $\|\beta^{J=1}\|$ being less than 7% of the octupolar one. Therefore the total quadratic hyperpolarizability (calculated from eq 1) is almost equal to $\|\beta^{J=3}\|$. The difference between the total quadratic hyperpolarizability and $\langle\beta_{\text{HLS}}\rangle$, β , is quite large ($876\text{--}916 \times 10^{-30}$ esu, Table 5) because $\langle\beta_{\text{HLS}}\rangle$ contains isotropic mean factors that decrease this parameter, as evidenced by the coefficients in eq 3.

Photochromic Behavior and Photoswitching of Optical Properties. The flexibility in the procedure for synthesizing the ligands readily allows the introduction of a photochromic dithienylethene for the elaboration of luminescent metallophotoswitches. The DTE-based bipyridine ligand **Le(o)** [(o) = open form; (c) = closed form] was used to prepare the cationic complex **2e(o)**. Irradiation of the open form **2e(o)** with UV light (350 nm) in a CH₂Cl₂ solution results in the appearance of a broad band at 715 nm in the electronic absorption spectrum, corresponding to the closed form **2e(c)** (Figure 8a). This characteristic low-energy band in the visible region can be attributed to the S₀ → S₁ transition of the closed-DTE unit. The corresponding band in the free ligand **Le(c)** is located at 669 nm: The bathochromic shift of 46 nm is due to the presence of the metal center acting as a Lewis acceptor. We have previously demonstrated the influence of an electron-donating terminal substituent (R) on the distal thiophene: Replacement of the terminal H atom by an amino group leads to a shift of 46 nm in the absorbance maximum of the low-energy band, from 623 nm (R = H) to 669 nm (R = NMe₂) (Table 6). These results illustrate the tuning of optical properties of the photochromic unit that are possible, thanks to the synthetic versatility of such systems.

¹H NMR spectroscopy can be used to estimate the proportion of open and closed forms in the photostationary state (PSS), as some of the signals of **2e(c)** are well-distinguished from those of **2e(o)**. For example, the signals of the methyl substituents of the thiophene groups (δ 2.18, 2.16) undergo a downfield shift, the dimethylamino group displays a signal at δ 3.11, whereas the singlet of methyl groups of the ppy ligand, remote from the DTE fragment, remains identical. The chemical conversion is relatively good (79%) showing that the complexation to the Ir(III) ion

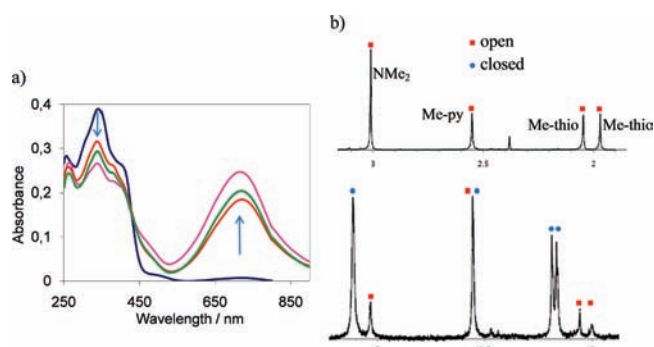


Figure 8. (a) UV-vis absorption changes of **2e** in CH₂Cl₂ (5×10^{-6} M) upon irradiation at 450 nm. (b) ¹H NMR spectra (CD₂Cl₂) of **2e**, before (top) and after (bottom) UV irradiation ($\lambda = 350$ nm, 10^{-3} M).

does not perturb too much the photochromic properties of **Le** (Figure 8b).

It is also interesting to note that the photochromic reaction can be triggered by irradiation of **2e** into the low-energy band at 410 nm. This MLCT photosensitization has been previously established for other metal complexes and suggests the intermediacy of the triplet state ³IL(DTE) in the photocyclization process. The intersystem crossing of ¹MLCT to triplet state ³MLCT is efficient for cyclometalated iridium complexes and allows an energy transfer to the lowest-lying open ³DTE state. Many photoswitchable metal complexes have been reported in the literature,¹⁵ but only two examples of heteroleptic bis-cyclometalated Ir(III) complexes containing two photochromic DTE units have been described up to now.²⁶ The fully closed isomer of multiphotochromic systems is, in many cases, not formed, behavior generally attributed to intramolecular energy transfer from the excited state to the lower-lying IL (closed-DTE) state.

The emission characteristics of complex **2e** are summarized in Table 6, and the emission spectrum is shown in Figure 9. As for complex **2d**, the excited state is assigned as a predominantly ³IL transition localized on the bpy-C=C-Ar moiety, with an energy similar to that of **2d** but with a shorter lifetime (23 versus 34 μ s), possibly indicative of some competitive quenching via the photocyclization pathway. This behavior contrasts with that of the free ligand **Le**, which is nonemissive at room temperature in fluid solution and even in frozen glasses at 77 K, suggesting that the rate of ring closure is faster in that case. Conversion of **2e(o)** to the PSS is accompanied by a substantial quenching of the 77 K luminescence (Figure 9), which can be attributed to intramolecular energy transfer from the triplet emissive state to the closing DTE part of the molecule: There is extensive overlap of the emission bands of the donor Ir luminophore ($\lambda_{\text{max}}^{\text{em}} = 650$ and 717 nm) with the low-energy absorption band of the acceptor photochromic unit in its closed form ($\lambda_{\text{max}}^{\text{abs}} = 715$ nm).

Table 6. Photophysical Characteristics of DTE-Based Ligand and Complexes

compound	$\lambda_{\text{abs}}/\text{nm}$ ($\epsilon/\text{M}^{-1} \text{cm}^{-1}$) ^a open	$\lambda_{\text{abs}}/\text{nm}$ ^a closed (PSS)	$\lambda_{\text{em}}/\text{nm}$ ($\tau/\mu\text{s}$) open	conversion % ^c
Le ^d	348 (89 000)	347, 395	no emission	95
(Le)Zn(OAc) ₂ ^d	360 (76 000)	343, 394	no emission	90
2e	304 (62 208), 341 (77 912), 397 (53 105)	263, 339	650, 717 (23)	79
		391, 715		

^a In CH₂Cl₂ at 298 K; PSS = photostationary state. ^b At 77 K in EPA (ether/isopentane/ethanol (2:2:1, v/v)); $\lambda_{\text{exc}} = 400 \text{ nm}$. ^c Determined by ¹H NMR spectroscopy. ^d From ref 13a.

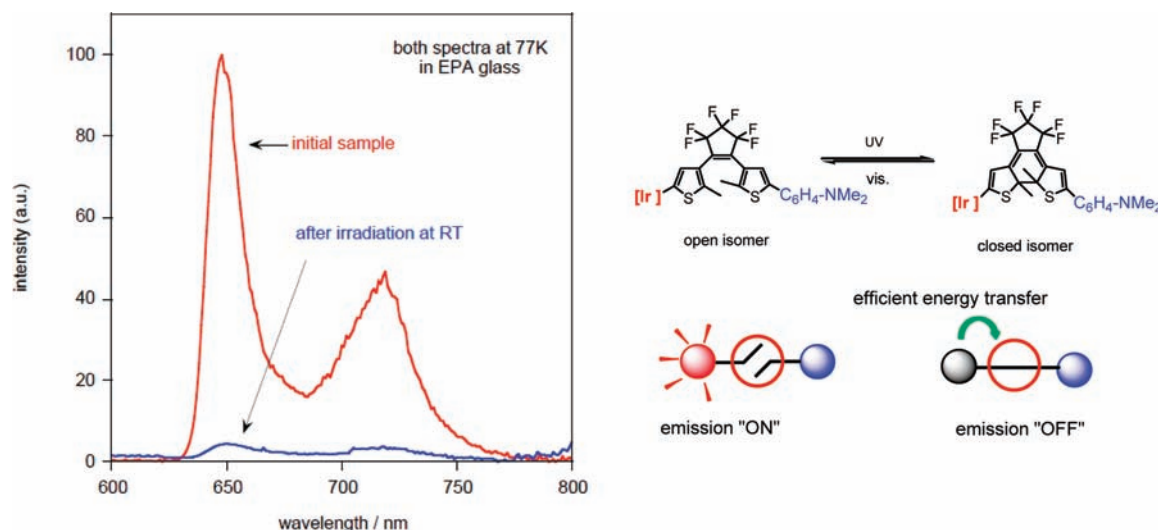


Figure 9. (Left panel) Emission spectra of open–open form and PSS (after broad-band irradiation $\sim 350 \text{ nm}$ of **2e** at 77 K in EPA. (Right panel) Schematic structure of the two forms of **2e**.

Finally, we have investigated the NLO response of **2e**[PF₆] in CH₂Cl₂ by the EFISH technique, at an incident wavelength of $1.907 \mu\text{m}$. Complex **2e(o)** gives rise to an EFISH $\mu\beta_{1,907}$ value of $-2190 \times 10^{-48} \text{ esu}$, comparable to that of the thienyl derivative **2d**. However, no significant modification of this value is observed after photocyclization [**2e(c)**: $-2000 \times 10^{-48} \text{ esu}$]. This absence of switching of the NLO response markedly contrasts with the huge enhancement of $\mu\beta_{1,907}$ observed for dipolar zinc(II) complexes featuring the same photochromic bipyridyl ligand.^{13a} The NLO responses of the Zn(II) complexes are governed by ILCT transitions involving the bipyridyl ligand, and the dramatic increase of the NLO activity in that case clearly reflects the efficient delocalization of the π -electron system in the closed form. In contrast, for the iridium(III) complexes **2a–e**, the negative EFISH hyperpolarizability is dominated by L'LCT/MLCT processes, and the nature of the π -conjugated substituents on the bipyridine ligand does not influence so much the $\mu\beta$ values (see Table 4).

CONCLUSIONS

We have presented in this work a full investigation on the synthesis, characterization, and linear and NLO properties of a new series of iridium(III) complexes [Ir(C^N-ppy-Me)₂(N^N-bpy-CH=CH-Ar-R)]⁺[X]⁻, which incorporate extended Ar-vinyl π systems on the bipyridine ligand. The systematic variation of end group R allows the modulation of their absorption and emission properties as supported by DFT and TD-DFT calculations.

Moreover the luminescence lifetimes τ , from 14 to 90 μs , are significantly affected due to the change of the nature of the emitting state (MLCT/L'LCT vs ILCT contribution).

We have also demonstrated that these cationic complexes display large second-order NLO responses which can be modulated by the nature of the substituents as well as by the concentration and nature of the counterion. The EFISH studies give high absolute $\mu\beta_{1,907}$ values, mainly controlled by MLCT/L'LCT processes from the cyclometalated phenylpyridine Ir(III) moiety to the π^* orbitals of the diimine. Moreover we have shown that ion pairing can affect the absolute $\mu\beta_{1,907}$ value, producing, when the ion pair is not too tight, a significant increase of the second-order NLO response. By analogy with related cationic 1,10-phenanthroline iridium(III) complexes, the origin of the increased NLO activity can be partly attributed to the decrease of the electronic perturbation induced by the counterion on the energy levels of the Ir(III) chromophore.^{12b}

The HLS NLO studies also show that both cationic 1,10-phenanthroline and bipyridine iridium(III) complexes are characterized by a large $\langle\beta_{1,907}\rangle$ value. The use of a combination of EFISH and HLS data demonstrates that, as previously observed in the case of cyclometalated Ln complexes,²⁴ the major contribution to the total quadratic hyperpolarizability is controlled mainly by the octupolar part. Such a major contribution to the quadratic hyperpolarizability is of particular interest because these complexes do not show the classical octupolar structure.

Finally, the incorporation of a photochromic DTE unit into the bipyridine ligand allows to switch ON and OFF the luminescence but not the NLO activity. Photocyclization can be triggered by using either UV or visible light, leading to an efficient quenching of luminescence; by contrast no significant modification of the EFISH $\mu\beta_{1.907}$ value is observed after photocyclization, confirming that the quadratic NLO response is dominated by MLCT/L⁺LCT processes and not by an ILCT transition.

EXPERIMENTAL SECTION

General Procedure. All manipulations were performed using Schlenk techniques under an Ar atmosphere. All solvents were dried and purified by standard procedures. NMR spectra were recorded on Bruker DPX-200, AV 300 or AV 500 MHz spectrometers. ¹H and ¹³C chemical shifts are given versus SiMe₄ and were determined by reference to residual ¹H and ¹³C solvent signals. Attribution of carbon atoms was based on heteronuclear multiple bonding connectivity (HMBC), heteronuclear multiple-quantum coherence (HMQC), and correlation spectroscopy (COSY) experiments. High-resolution mass spectra (HRMS) were performed on a MS/MS ZABSpec TOF at the Centre de Mesures Physiques de l'Ouest (CRMPO) in Rennes. Elemental analyses were performed at the CRMPO. UV–vis absorption spectra were recorded using a UVIKON 9413 or Biotek Instruments XS spectrophotometer using quartz cuvettes of 1 cm path length. Steady-state luminescence spectra were measured using a Jobin Yvon Fluor-oMax-2 or Tau-3 spectrofluorimeter, fitted with a red-sensitive Hamamatsu R928 photomultiplier tube. The spectra shown are corrected for the wavelength dependence of the detector, and the quoted emission maxima refer to the values after correction. Lifetimes were obtained by multichannel scaling following excitation with a μ s-pulsed xenon lamp and detection of the light emitted at right angles using an R928 photomultiplier tube, after passage through a monochromator. Dipole moments μ were measured in CHCl₃ by using a WTW-DM01 dipolemeter (dielectric constant) coupled with a RX-5000 ATAGO digital refractometer (refractive index) according to the Guggenheim method.²²

DFT Calculations. The geometries of all compounds have been fully optimized using the PBE0 functional²⁷ and the LANL2DZ basis set augmented with polarization functions on all atoms, except hydrogen ones with the Gaussian03 program.²⁸ The computations of the electronic absorption spectra were carried out using TD-DFT at the same level of theory with the same Gaussian03 package, utilizing the previously optimized ground-state geometries. The TD-DFT calculations took into account a minimum of 20 excited states, leading to the consideration of more than 6 occupied and 6 virtual MOs; the corresponding variational space was found sufficiently large to obtain a perfectly converged computed spectra in the visible and UV regions. Representation of molecular structures and orbitals was done using the Molekel program,²⁹ while theoretical absorption spectra were plotted using Swizard,³⁰ the half-bandwidths for the Gaussian model being taken equal to 3500 cm⁻¹.

EFISH Measurements. The molecular quadratic hyperpolarizabilities of all the investigated complexes (Table 4) were measured by the solution phase dc EFISH generation method,³¹ which can provide direct information on the intrinsic molecular NLO properties through eq 4:

$$\gamma_{\text{EFISH}} = (\mu\beta_{\lambda}/SkT) + \gamma(-2\omega; \omega, \omega, 0) \quad (4)$$

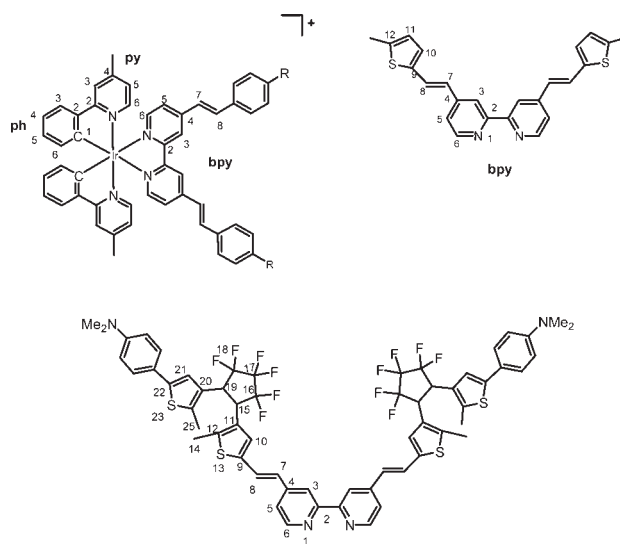
where $\mu\beta_{\lambda}/SkT$ is the dipolar orientational contribution, and $\gamma(-2\omega; \omega, \omega, 0)$, a third-order term corresponding to the mixing of two optical fields at ω and of the DC poling field at $\omega = 0$, is the electronic cubic contribution to γ_{EFISH} which is usually negligible. β_{λ} is the projection along the dipole moment axis of the vectorial component of the tensor of the quadratic hyperpolarizability, working with an incident wavelength λ .

All EFISH measurements were carried out at the Dipartimento di Chimica Inorganica Metallorganica e Analitica "Lamberto Malatesta" of

the Università degli Studi di Milano, in CH₂Cl₂ solutions at a concentration of 1×10^{-4} and 1×10^{-3} M, working with a nonresonant incident wavelength of 1.907 μ m, obtained by Raman shifting the fundamental 1.064 μ m wavelength produced by a Q-switched, mode-locked Nd³⁺:YAG laser manufactured by Atalaser. The apparatus for the EFISH measurements was a prototype made by SOPRA (France). The $\mu\beta_{\text{EFISH}}$ values reported are the mean values of 16 successive measurements performed on the same sample.

HLS Measurements. The HLS technique^{25,32} involves the detection of the incoherently scattered second harmonic generated by a solution of the molecule under irradiation with a laser of wavelength λ , leading to the measurement of the mean value of the $\beta \times \beta$ tensor product, $\langle\beta_{\text{HLS}}\rangle$. All HLS measurements were carried out at the École Normale Supérieure de Cachan in CH₂Cl₂ or deuterated DMF²³ solutions at a concentration of 1×10^{-3} M, working with a low-energy nonresonant incident radiation of 1.907 μ m.

Atom numbering scheme for NMR assignments:



Preparation of **Ld.** In a Schlenk tube, 5-methylthiophene-2-carbaldehyde (0.54 mL, 5 mmol) and 4,4'-bis(diethylphosphonomethyl)-2,2'-bipyridine (0.912 mg, 2 mmol) were dissolved in 80 mL of THF, then ^tBuOK (0.56 mg, 5 mmol) was added. The reaction mixture was heated under reflux 4 h. The product was precipitated by addition of water (10 mL) and washed with pentane and acetone. The yellow powder was dried under vacuum (0.537 g, 67%). ¹H NMR (500 MHz, CD₂Cl₂): 8.64 (d, *J* = 5.2 Hz, 2H, H⁶-bpy), 8.54 (s, 2H, H³-bpy), 7.57 (d, ³*J* = 16 Hz, 2H, =CH⁸), 7.37 (dd, ³*J* = 5.1 Hz, ⁴*J* = 1.7 Hz, H⁵-bpy), 7.04 (d, ³*J* = 3.5 Hz, 2H, H¹⁰-thio), 6.87 (d, ³*J* = 16 Hz, 2H, =CH⁷), 6.76 (dd, ³*J* = 3.5 Hz, ⁴*J* = 1.1 Hz, 2H, H¹¹-thio), 2.54 (s, 6H, CH₃-thio). ¹³C [¹H] NMR (75.4 MHz, CD₂Cl₂): 156.4 (bpy²), 149.5 (bpy⁶), 145.5 (bpy⁴), 141.4 (C¹²-thio), 139.7 (C⁹-thio), 128.5 (C¹⁰-thio), 126.5 (=CH), 126.1 (C¹¹-thio), 124.2 (=CH), 120.5 (bpy⁵), 117.6 (bpy³), 15.5 (Me). Anal. calcd for C₂₄H₂₀N₂S₂: C, 71.96; H, 5.03; N, 6.99. Found: C, 71.64; H, 5.10; N, 7.00.

Syntheses of Cationic Complexes [Ir(C^N-ppy-R)(N^N)]⁺[X⁻] (X⁻ = PF₆⁻, C₁₂H₂₅SO₃⁻). A Schlenk flask was charged with the dimer [Ir(C^N-ppy-R)₂](μ-Cl)₂ (R = Me, C₆H₁₃) AgPF₆ (1 equiv) or NaC₁₂H₂₅SO₃ (2.5 equiv) and the appropriate ligand N^N, **1** (3.5 equiv) and 10 mL of CH₂Cl₂. The mixture was stirred for 2–3 h. The solvent was evaporated, and the residue washed with Et₂O (2 × 20 mL). Recrystallization in a mixture of CH₂Cl₂/Et₂O gave the cationic complex.

[2d][PF₆]. Yellow powder, yield 66%. ¹H NMR (300 MHz, CD₂Cl₂): 8.58 (s, 2H, H³-bpy), 7.87 (d, ³J = 6 Hz, 2H, H⁶-bpy), 7.80 (s, 2H, H³-py), 7.78 (d, ³J = 16 Hz, 2H, =CH⁸), 7.76 (d, ³J = 6.7 Hz, 2H, H³-Ph), 7.45 (d, ³J = 6 Hz, 2H, H⁶-py), 7.39 (dd, ³J = 5.8 Hz, 2H, H⁵-bpy), 7.23 (d, ³J = 3.5 Hz, 2H, thio¹⁰), 7.10 (td, ³J = 7.5 Hz, ⁴J = 1.0 Hz, 2H, H¹-Ph), 6.95 (td, ³J = 7.5 Hz, 2H, H⁵-Ph), 6.91 (d, ³J = 18 Hz, 2H, =CH⁷), 6.86 (td, ³J = 6 Hz, 2H, H⁵-py), 6.80 (d, ³J = 3.5 Hz, 2H, thio¹¹), 6.38 (d, ³J = 7.0 Hz, 2H, H⁶-Ph), 2.56 (s, 6H, CH₃thio), 2.54 (s, 6H, CH₃py). ¹³C [¹H] NMR (75 MHz, CD₂Cl₂): 167.1 (C²-py), 156.0 (C²-bpy), 150.8 (C¹-Ph), 150.2 (C⁴-py), 150.1 (C⁶-bpy), 148.0 (C⁴-bpy), 147.8 (C⁶-py), 143.83, 143.79 (C²-Ph, thio¹²), 138.6 (thio⁹), 131.7 (C⁶-Ph), 131.0 (thio¹⁰), 130.6 (=CH), 130.3 (C⁵-Ph), 126.7 (thio¹¹), 124.5 (C³-Ph), 124.3 (C⁵-bpy), 123.8 (C⁵-py), 122.4 (C⁴-Ph), 120.7 (C³-bpy), 120.4 (C³-py), 121.2 (=CH), 21.1 (CH₃py), 15.6 (CH₃thio). Anal. calcd for C₄₈H₄₀F₆N₄PS₂: C, 53.67; H, 3.75; N, 5.22. Found: C, 54.03; H, 3.76; N, 5.08.

[2b][PF₆]. Yellow powder, yield 85%. ¹H NMR (300 MHz, CD₂Cl₂): 8.71 (s, 2H, bpy³), 7.87 (d, ³J = 5.85 Hz, 2H, bpy⁶), 7.80 (s, 2H, py³), 7.75 (dd, ³J = 7.9 Hz, ⁴J = 0.95 Hz, 2H, Ph³), 7.67 (d, ³J = 8.8 Hz, 4H, C₆H₄), 7.63 (d, ³J = 16.3 Hz, 2H, =CH), 7.46 (m, 4H, py⁶, bpy⁵), 7.23 (d, ³J = 16.3 Hz, 2H, =CH), 7.09 (td, ³J = 7.6 Hz, ⁴J = 1.1 Hz, 2H, Ph⁴), 6.97 (d, ³J = 8.8 Hz, 4H, C₆H₄), 6.95 (td, ³J = 7.4 Hz, ⁴J = 1.3 Hz, 2H, Ph⁵), 6.86 (td, ³J = 6.3 Hz, ⁴J = 1.6 Hz, 2H, py⁵), 6.38 (dd, ³J = 7.6 Hz, ⁴J = 0.8 Hz, 2H, Ph⁶), 4.03 (t, ³J = 6.6 Hz, 4H, CH₂), 2.54 (s, 6H, CH₃-py), 1.82 (q, ³J = 7.1 Hz, 4H, CH₂), 1.50 (q, ³J = 8.0 Hz, 4H, CH₂), 1.31–1.40 (m, 16H, CH₂), 0.93 (s, 6H, CH₃). ¹³C [¹H] NMR (75 MHz, CD₂Cl₂): 167.1 (py²), 160.7 (C₆H₄^{para}), 156.1 (bpy²), 151.0 (Ph¹), 150.1 (py⁴), 149.9 (bpy⁶), 148.6 (bpy⁴), 147.8 (py⁶), 143.9 (Ph²), 136.9 (=CH⁸), 131.7 (Ph⁶), 130.3 (Ph⁵), 129.3 (C₆H₄^{ortho}), 128.0 (C₆H₄^{ipso}), 124.5 (Ph³), 124.3 (py⁵), 123.6 (bpy⁵), 122.3 (Ph⁴), 121.4 (bpy³), 121.2 (=CH⁷), 120.4 (py³), 114.9 (C₆H₄^{meta}), 68.2 (C¹⁶), 31.8 (C^{19–22}), 29.3 (C^{19–22}), 29.2 (C^{19–22}), 29.1 (C¹⁸), 26.0 (C¹⁷), 22.6 (C^{19–22}), 21.0 (CH₃-py), 13.9 (C²³). HRMS (*m/z*): 1145.52847 [M]⁺ calcd for C₆₆H₇₂N₄O₂¹⁹³Ir, 1145.5290. Anal. calcd for C₆₆H₇₂F₆IrN₄O₂P: C, 61.43; H, 5.62; N, 4.34. Found: C, 61.20; H, 5.64; N, 4.31.

[2a][PF₆]. Red powder, yield 87%. ¹H NMR (300 MHz, CD₂Cl₂): 8.41 (s, 2H, bpy³), 7.82 (d, ³J = 6 Hz, 2H, bpy⁶), 7.81 (s, 2H, py³), 7.76 (d, ³J = 7.8 Hz, ⁴J = 0.9 Hz, 2H, Ph³), 7.55 (d, ³J = 8.9 Hz, 2H, C₆H₄), 7.52 (d, ³J = 16 Hz, 2H, =CH), 7.47 (d, ³J = 6 Hz, 2H, py⁶), 7.42 (dd, ³J = 6.1 Hz, ⁴J = 1.5 Hz, 2H, bpy⁵), 7.07 (td, ³J = 7.6 Hz, ⁴J = 1.0 Hz, 2H, Ph⁴), 7.05 (d, ³J = 16.3 Hz, 2H, =CH), 6.96 (td, ³J = 7.3 Hz, ⁴J = 1.1 Hz, 2H, Ph⁵), 6.86 (td, ³J = 6 Hz, ⁴J = 1.4 Hz, 2H, py⁵), 6.74 (d, ³J = 8.6 Hz, 2H, C₆H₄), 6.40 (d, ³J = 7.5 Hz, 2H, Ph⁶), 3.46 (m, 8H, CH₂), 2.55 (s, 6H, CH₃py), 1.24 (t, ³J = 7.0 Hz, 6H, CH₃). ¹³C [¹H] NMR (75 MHz, CD₂Cl₂): 167.2 (py²), 155.9 (bpy²), 151.1 (Ph¹), 150.0 (py⁴), 149.9 (bpy⁶), 148.9 (C¹²), 177.7 (py⁶), 143.9 (Ph²), 137.6 (=CH), 137.9 (bpy⁴), 131.7 (Ph⁶), 130.3 (Ph⁵), 129.6 (C₆H₄), 124.5 (Ph³), 124.2 (py⁵), 123.0 (bpy⁵), 122.3 (Ph⁴), 122.1 (C₆H₄), 122.3 (cipso), 120.4 (py³), 120.2 (bpy³), 117.4 (=CH), 111.4 (C₆H₄), 44.5 (CH₂), 21.1 (CH₃py), 12.3 (CH₃). HRMS (*m/z*): 1029.4345 [M]⁺ calcd for C₅₈H₁₁₆N₆Ir, 1029.43290.

[2a][C₁₂H₂₅SO₃]. ¹H NMR (500 MHz, CD₂Cl₂): 8.92 (s, 2H, bpy³), 7.79 (s, 2H, py³), 7.78 (d, ³J = 5.9 Hz, 2H, bpy⁶), 7.75 (d, ³J = 7.9 Hz, 2H, Ph³), 7.68 (d, ³J = 16.2 Hz, 2H, =CH⁸), 7.62 (d, ³J = 8.8 Hz, 4H, C₆H₄^{ortho}), 7.50 (d, ³J = 6.0 Hz, 2H, py⁶), 7.39 (d, ³J = 5.9 Hz, 2H, bpy⁵), 7.16 (s, 2H, ³J = 16.2 Hz, 2H, =CH⁷), 7.09 (t, ³J = 7.5 Hz, 2H, Ph⁴), 6.95 (t, ³J = 7.5 Hz, 2H, Ph⁵), 6.86 (d, ³J = 6.0 Hz, 2H, py⁵), 6.74 (d, ³J = 8.8 Hz, 4H, C₆H₄^{meta}), 6.39 (d, ³J = 7.6 Hz, 2H, Ph⁶), 3.45 (m, 8H, CH₂[NEt₂]), 2.78 (m, 2H, CH₂¹[C₁₂H₂₅SO₃⁻]), 2.54 (s, 6H, CH₃^{py}), 1.82 (m, 2H, CH₂²[C₁₂H₂₅SO₃⁻]), 1.23 (m, 30H, CH₃[NEt₂] + CH₂^{3–11}[C₁₂H₂₅SO₃⁻]), 0.91 (m, 3H, CH₃[C₁₂H₂₅SO₃⁻]).

Preparation of ppy-C₆H₁₃. To a solution of diisopropylamine (0.30 mL, 2.11 mmol) and butyllithium (1.2 mL [1.60 M], 1.94 mmol) in 10 mL of THF, was added 4-methyl-2-phenylpyridine (300 mg, 1.76 mmol)

at –78 °C. After 1 h of stirring, 1-iodopentane (523 mg, 2.65 mmol) was added via a syringe, and the reaction was stirred at room temperature for 15 h. After addition of a NaHCO₃ solution (20 mL), the product was extracted with dichloromethane (3 × 20 mL). The organic phase was washed with brine. Evaporation of the solvents gave a brown oil (378 mg, yield 91%). ¹H NMR (500 MHz, CDCl₃): 8.59 (dd, 1H, ³J = 5.0 Hz, ⁴J = 0.6 Hz, py⁶), 8.00 (m, 2H, Ph^{ortho}), 7.57 (d, 1H, ⁴J = 0.7 Hz, py³), 7.50 (m, 2H, Ph^{meta}), 7.45 (m, 1H, Ph^{para}), (dd, 1H, ³J = 5.0 Hz, ⁴J = 1.55 Hz, py⁵), 2.69 (m, 2H, CH₂), 1.70 (m, 2H, CH₂), 1.36 (m, 6H, (CH₂)₃), 0.92 (m, 3H, CH₃).

Preparation of the Dimer [Ir(C^N-ppy-C₆H₁₃)₂](μ-Cl)₂. In a Schlenk tube, 4-hexyl-2-phenylpyridine (378 mg, 1.6 mmol) and IrCl₃·3 H₂O (159 mg, 0.53 mmol) were dissolved in 15 mL of a mixture of 2-ethoxyethanol/water (75/25). The reaction was heated at 140 °C for 24 h. The product was extracted with dichloromethane, and the organic phase was washed with water. Evaporation of the solvent gave a yellow powder (164 mg, Yield: 44%). ¹H NMR (500 MHz, CD₂Cl₂): 9.14 (d, 1H, ³J = 6.0 Hz, py⁶), 7.79 (d, 1H, ⁴J = 1.7 Hz, py³), 7.58 (dd, 1H, ³J = 7.8 Hz, ⁴J = 1.4 Hz, Ph³), 6.84 (td, 1H, ³J = 7.4 Hz, ⁴J = 1.1 Hz, Ph⁴), 6.69 (dd, 1H, ³J = 6.0 Hz, ⁴J = 1.9 Hz, py⁵), 6.65 (td, 1H, ³J = 7.5 Hz, ⁴J = 1.4 Hz, Ph⁵), (dd, 1H, ³J = 7.8 Hz, ⁴J = 0.9 Hz, Ph⁶), 2.92 (m, 2H, CH₂), 1.89 (m, 2H, CH₂), 1.57 (m, 2H, CH₂), 1.48 (m, 4H, (CH₂)₂), 0.92 (m, 3H, CH₃). HRMS (*m/z*): 1408.5038 [M]⁺ calcd for C₆₈H₈₀N₄Cl₂Ir₂, 1408.50189. Anal. calcd for C₆₈H₈₀N₄Cl₂Ir₂: C, 57.98; H, 5.72; N, 3.98. Found: C, 57.82; H, 5.86; N, 3.97.

[2c][PF₆]. Red powder, yield 69%. ¹H NMR (500 MHz, CD₂Cl₂): 8.98 (s, 1H, bpy³), 8.25 (d, ³J = 8.9 Hz, 2H, C₆H₄), 7.99 (d, ³J = 5.8 Hz, 1H, bpy⁶), 7.90 (d, ³J = 8.9 Hz, 2H, C₆H₄), 7.82 (d, ⁴J = 1.54 Hz, 1H, py³), 7.79 (dd, ³J = 7.95 Hz, ⁴J = 1.02 Hz, 1H, Ph³), 7.77 (d, ³J = 16.4 Hz, 1H, =CH), 7.53 (d, ³J = 5.9 Hz, 1H, bpy⁵), 7.54 (d, ³J = 16.4 Hz, 1H, =CH), 7.49 (d, ³J = 6.0 Hz, 1H, py⁶), 7.12 (td, ³J = 7.6 Hz, ⁴J = 1.1 Hz, 1H, Ph⁴), 6.98 (td, ³J = 7.4 Hz, ⁴J = 1.3 Hz, 1H, Ph⁵), 6.89 (dd, ³J = 6.08 Hz, ⁴J = 1.86 Hz, 1H, Py⁵), 6.38 (dd, ³J = 7.5 Hz, ⁴J = 0.9 Hz, 1H, Ph⁶), 2.78 (m, 2H, CH₂), 1.70 (m, 2H, CH₂), 1.39 (m, 2H, CH₂), 1.34 (m, 4H, (CH₂)₂), 0.90 (m, 3H, CH₃). ¹³C [¹H] NMR (75 MHz, CD₂Cl₂): 167.08 (py²), 156.43 (bpy²), 154.90 (py⁴), 150.56 (Ph¹), 150.43 (bpy⁶), 147.95 (C₆H₄^{para}), 147.90 (Py⁶), 147.20 (bpy⁴), 143.96 (Ph²), 141.96 (C₆H₄^{ipso}), 134.51 (=CH⁸), 131.73 (Ph⁶), 130.36 (Ph⁵), 128.38 (2xC₆H₄^{ortho}), 128.05 (=CH⁷), 124.66 (bpy⁵), 124.56 (Ph³), 124.05 (2xC₆H₄^{meta}), 123.68 (bpy⁵), 122.52 (bpy³), 122.48 (Ph⁴), 119.75 (py³), 35.36 (CH₂¹), 31.51 (CH₂^{4/5}), 30.12 (CH₂²), 28.84 (CH₂³), 22.49 (CH₂^{4/5}), 13.77 (CH₃).

[2c][C₁₂H₂₅SO₃]. Red powder, yield 76%. ¹H NMR (500 MHz, CD₂Cl₂): 9.95 (s, 2H, bpy³), 8.39 (d, ³J = 16.5 Hz, 2H, =CH), 8.28 (d, ³J = 8.9 Hz, 4H, C₆H₄), 8.10 (d, ³J = 8.8 Hz, 4H, C₆H₄), 7.94 (d, ³J = 5.7 Hz, 2H, bpy⁶), 7.82 (m, 4H, py³, Ph³), 7.75 (d, ³J = 16.5 Hz, 2H, =CH), 7.53 (m, 4H, bpy⁵, py⁶), 7.10 (td, ³J = 7.6 Hz, ⁴J = 1.1 Hz, 2H, Ph⁴), 6.97 (td, ³J = 7.4 Hz, ⁴J = 1.2 Hz, 2H, Ph⁵), 6.89 (dd, ³J = 6; 1 Hz, ⁴J = 1.8 Hz, 2H, Py⁵), 6.38 (dd, ³J = 7.5 Hz, ⁴J = 0.8 Hz, 2H, Ph⁶), 2.85 (2H, CH₂¹[C₁₂H₂₅SO₃⁻]), 2.78 (t, ³J = 7.70 Hz, 4H, CH₂), 1.85 (m, 2H, CH₂²[C₁₂H₂₅SO₃⁻]), 1.70 (m, 4H, CH₂[py]), 1.30 (m, 30H, CH₂), 0.90 (m, 9H, CH₃[py] + CH₃[C₁₂H₂₅SO₃⁻]). Anal. calcd for C₇₂H₈₈N₆O₆SiR·0.5CH₂Cl₂: C, 61.70; H, 6.00; N, 5.96; S, 2.27. Found: C, 61.59; H, 5.96; N, 5.88; S, 1.48.

[2e(o)][PF₆](open form). Yellow-brown powder, yield 75%. ¹H NMR (500 MHz, CD₂Cl₂): 8.62 (s, 2H, bpy³), 7.90 (d, ³J = 5.8 Hz, 2H, bpy⁶), 7.80 (s, 2H, py³), 7.76 (d, 2H, Ph³), 7.70 (d, ³J = 16.4 Hz, 2H, =CH⁸), 7.45 (d, ³J = 8.68 Hz, 4H, C₆H₄), 7.44 (m, 4H, bpy⁵, py⁶), 7.38 (s, 2H, thio¹⁰), 7.15 (s, 2H, thio¹¹), 7.10 (t, ³J = 7.3 Hz, 2H, Ph⁴), 7.03 (d, 2H, =CH⁷), 6.95 (t, ³J = 6.32 Hz, 2H, Ph⁵), 6.86 (d, ³J = 5.82, 2H, py⁵), 6.75 (d, 4H, C₆H₄), 6.37 (d, ³J = 7.4 Hz, 2H, Ph⁶), 3.10 (s, 12H, NMe₂), 2.55 (s, 6H, Mepy), 2.07 (s, 6H, Me¹⁴), 2.04 (s, 6H, Me²⁵). ¹³C [¹H] NMR (75 MHz, CD₂Cl₂): 167.1 (py²), 156.1 (bpy²), 150.6 (Ph¹), 150.4 (C₆H₄^{para}), 150.3 (bpy⁶ + py⁴), 147.8 (py⁶), 147.5 (bpy⁴), 145.0

(thio¹²), 143.8 (Ph²), 143.5 (thio²²), 139.4 (thio²⁴), 138.9 (thio⁹), 131.7 (Ph⁶), 130.4 (Ph⁵), 129.8 (thio¹⁰), 129.3 (=CH⁸), 126.4 (C₆H₄^{ortho}), 126.1 (thio¹¹), 125.2 (thio²⁰), 124.6 (Ph³), 124.3 (py⁵), 123.8 (bpy⁵), 123.2 (=CH⁷), 122.5 (Ph⁴), 121.3 (bpy³), 121.2 (C₆H₄^{isps}), 120.4 (py³), 119.4 (thio²¹), 112.2 (C₆H₄^{meta}), 40.1 (NMe₂), 21.1 (CH₃-py), 14.8 (CH₃¹⁴), 14.3 (CH₃²⁵). HRMS (*m/z*): 1705.3714 [M]⁺ calcd for C₈₄H₆₆N₆F₁₂S₄¹⁹¹Ir, 1705.36463. Anal. calcd for C₈₄H₆₆F₁₈N₆PS₄Ir · 3 CH₂Cl₂: C, 49.58; H, 3.44; N, 3.99. Found: C, 49.86; H, 3.66; N, 4.00.

Spectroscopic Data of the Photocyclized Closed–Closed Isomer 2e(c). A solution of 2e(o) (5 mg) in 0.5 mL of CD₂Cl₂ was irradiated (λ = 350 nm) in an NMR tube for 24 h, giving rise to a green color. The rate of 79% conversion was determined on the basis of the integration of the methyl (thiophene) signals. Selected ¹H NMR data (500 MHz, CD₂Cl₂): 7.93 (d, ³*J* = 5.8 Hz, 2H, bpy⁶), 6.64 (s, 1H, thio), 3.11 (s, 12H, NMe₂), 2.18 (s, 6H, Me¹⁴), 2.16 (s, 6H, Me²⁵).

ASSOCIATED CONTENT

Supporting Information. UV–vis absorption spectra of **Le(c)** and **2e(c)** (PSS); excitation and emission spectra of **2e(o)** at 77 K emission spectra, energy (eV) of the molecular orbitals and contribution (%) of the metal (5d-Ir) of Ir complexes **2a,c,d** and **3**; details of DFT and TD-DFT calculations on complexes **2a,c,d** and **3**. This material is available free of charge via the Internet at <http://pubs.acs.org>.

AUTHOR INFORMATION

Corresponding Author

*E-mail: veronique.guerchais@univ-rennes1.fr (V.G.), dominique.roberto@unimi.it (D.R.).

ACKNOWLEDGMENT

This work is supported by ANR-08-BLAN-0112-01 no (COMET), COST D035-0010-05, and MIUR (FIRB 2004: RBPR-05JH2P and PRIN 2008: 2008FZKSAC_002). We deeply thank Prof. Alceo Macchioni (University of Perugia) for PGSE NMR investigations and CNRS (PICS Rennes (F)-Durham (UK)) and the University of Rennes1 for financial support.

REFERENCES

- (1) (a) Yersin, H. *Highly Efficient OLEDs with Phosphorescent Materials*; Wiley-VCH: Berlin, Germany, 2007. (b) Coe, B. J. In *Comprehensive Coordination Chemistry II*; Elsevier Pergamon: Oxford, U.K., 2004; Vol. 9. (c) Coe, B. J.; Curati, N. R. M. *Comments Inorg. Chem.* **2004**, *25*, 147–184. (d) Maury, O.; Le Bozec, H. *Acc. Chem. Res.* **2005**, *38*, 691–704. (e) Powell, C. E.; Humphrey, M. G. *Coord. Chem. Rev.* **2004**, *248*, 725–756. (f) Cariati, E.; Pizzotti, M.; Roberto, D.; Tessore, F.; Ugo, R. *Coord. Chem. Rev.* **2006**, *250*, 1210–1233. (g) Coe, B. J. *Acc. Chem. Res.* **2006**, *39*, 383–393. (h) Humphrey, M. G.; Samoc, M. *Adv. Organomet. Chem.* **2007**, *55*, 61–136. (i) Di Bella, S.; Dragonetti, C.; Pizzotti, M.; Roberto, D.; Tessore, F.; Ugo, R. In *Topics in Organometallic Chemistry 28. Molecular Organometallic Materials for Optics*; Le Bozec, H., Guerchais, V., Eds.; Springer: Heidelberg, Germany, 2010; Vol. 28, pp 1–55. (j) Liu, Z.; Bian, Z.; Huang, C. In *Topics in Organometallic Chemistry: Molecular Organometallic Materials for Optics*; Le Bozec, H., Guerchais, V., Eds.; Springer: Heidelberg, Germany, 2010; Vol. 28, pp 113–142.
- (2) (a) Baldo, M. A.; Lamansky, S.; Burrows, P. E.; Thompson, M. E.; Forrest, S. R. *Appl. Phys. Lett.* **1999**, *75*, 4–6. (b) Dedeian, K.; Djurovich, P. I.; Garces, F. O.; Carlson, G.; Watts, R. J. *Inorg. Chem.* **1991**, *30*, 1685–1687. (c) Zhou, G. J.; Wong, W. Y.; Yao, B.; Xie, Z. Y.; Wang, L. X. *Angew. Chem., Int. Ed.* **2007**, *46*, 1149–1151. (d) Tsuboyama,

- A.; Iwawaki, H.; Furugori, M.; Mukaide, T.; Kamatani, J.; Igawa, S.; Moriyama, T.; Miura, S.; Takiguchi, T.; Okada, S.; Hoshino, M.; Ueno, K. *J. Am. Chem. Soc.* **2003**, *125*, 12971–12979. (e) Okada, S.; Okinaka, K.; Iwawaki, H.; Furugori, M.; Hashimoto, M.; Mukaide, T.; Kamatani, J.; Igawa, S.; Tsuboyama, A.; Takiguchi, T.; Ueno, K. *Dalton Trans.* **2005**, 15831590. (f) Adachi, C.; Baldo, M. A.; Forrest, S. R.; Thompson, M. E. *Appl. Phys. Lett.* **2000**, *77*, 904–906. (g) Blumstengel, S.; Meinardi, F.; Tubino, R.; Gurioli, M.; Jandke, M.; Strohrriegel, P. *J. Chem. Phys.* **2001**, *115*, 3249–3255. (h) Grushin, V. V.; Herron, N.; LeCloux, D. D.; Marshall, W. J.; Petrov, V. A.; Wang, Y. *Chem. Commun.* **2001**, 1494–1495. (i) Adamovich, V.; Brooks, J.; Tamayo, A.; M. Alexander, A.; Djurovich, P. I.; D’Andrade, B. W.; Adachi, C.; Forrest, S. R.; Thompson, M. E. *New J. Chem.* **2002**, *26*, 1171–1178. (j) Tamayo, A. B.; Alleyne, B. D.; Djurovich, P. I.; Lamansky, S.; Tsyba, I.; Ho, N. N.; Bau, R.; Thompson, M. E. *J. Am. Chem. Soc.* **2003**, *125*, 7377–7387. (k) King, K. A.; Spellane, P. J.; Watts, R. J. *J. Am. Chem. Soc.* **1985**, *107*, 1431–1432. (l) Colombo, M. G.; Brunold, T. C.; Riedener, T.; Gudel, H. U.; Fortsch, M.; Burgi, H. B. *Inorg. Chem.* **1994**, *33*, 545–550. (m) Brunner, K.; van Dijken, A.; Borner, H.; Bastiaansen, J.; Kiggen, N. M. M.; Langeveld, B. M. W. *J. Am. Chem. Soc.* **2004**, *126*, 6035–6042.
- (3) Lamansky, S.; Djurovich, P.; Murphy, D.; Abdel-Razzaq, F.; Lee, H. E.; Adachi, C.; Burrows, P. E.; Forrest, S. R.; Thompson, M. E. *J. Am. Chem. Soc.* **2001**, *123*, 4304–4312.
- (4) (a) Adachi, C.; Baldo, M. A.; Forrest, S. R.; Lamansky, S.; Thompson, M. E.; Kwong, R. C. *Appl. Phys. Lett.* **2001**, *78*, 1622–1624. (b) Adachi, C.; Baldo, M. A.; Thompson, M. E.; Forrest, S. R. *J. Appl. Phys.* **2001**, *90*, 5048–5051. (c) Adachi, C.; Kwong, R. C.; Djurovich, P.; Adamovich, V.; Baldo, M. A.; Thompson, M. E.; Forrest, S. R. *Appl. Phys. Lett.* **2001**, *79*, 2082–2084. (d) Ikai, M.; Tokito, S.; Sakamoto, Y.; Suzuki, T.; Taga, Y. *Appl. Phys. Lett.* **2001**, *79*, 156–158. (e) Lamansky, S.; Djurovich, P.; Murphy, D.; Abdel-Razzaq, F.; Kwong, R.; Tsyba, I.; Bortz, M.; Mui, B.; Bau, R.; Thompson, M. E. *Inorg. Chem.* **2001**, *40*, 1704–1711. (f) Duan, J. P.; Sun, P. P.; Cheng, C. H. *Adv. Mater.* **2003**, *15*, 224–228. (g) Holmes, R. J.; D’Andrade, B. W.; Forrest, S. R.; Ren, X.; Li, J.; Thompson, M. E. *Appl. Phys. Lett.* **2003**, *83*, 3818–3820. (h) Su, Y. J.; Huang, H. L.; Li, C. L.; Chien, C. H.; Tao, Y. T.; Chou, P. T.; Datta, S.; Liu, R. S. *Adv. Mater.* **2003**, *15*, 884–888. (i) Tokito, S.; Iijima, T.; Tsuzuki, T.; Sato, F. *Appl. Phys. Lett.* **2003**, *83*, 2459–2461. (j) Coppo, P.; Plummer, E. A.; De Cola, L. *Chem. Commun.* **2004**, 1774–1775.
- (5) (a) Lo, K. K. W.; Ng, D. C. M.; Chung, C. K. *Organometallics* **2001**, *20*, 4999–5001. (b) Lo, K. K. W.; Chung, C. K.; Lee, T. K. M.; Lui, L. H.; Tsang, K. H. K.; Zhu, N. Y. *Inorg. Chem.* **2003**, *42*, 6886–6897. (c) Lo, K. K. W.; Chung, C. K.; Zhu, N. Y. *Chem.—Eur. J.* **2003**, *9*, 475–483. (d) Lo, K. K.-W.; Chung, C.-K.; Zhu, N. Y. *Chem.—Eur. J.* **2006**, *12*, 1500–1512. (e) Lo, K. K.-W.; Zhang, K. Y.; Chung, C. K.; Kwok, K. Y. *Chem.—Eur. J.* **2007**, *13*, 7110–7120. (f) Lo, K. K. W.; Zhang, K. Y.; Leung, S. K.; Tang, M. C. *Angew. Chem., Int. Ed.* **2008**, *47*, 2213–2216. (g) Lau, J. S.-Y.; Lee, P.-K.; Tsang, K. H.-K.; Ng, C. H.-C.; Lam, Y.-W.; Cheng, S.-H.; Lo, K. K.-W. *Inorg. Chem.* **2009**, *48*, 708–719.
- (6) (a) Colombo, M. G.; Gudel, H. U. *Inorg. Chem.* **1993**, *32*, 3081–3087. (b) Colombo, M. G.; Hauser, A.; Gudel, H. U. *Inorg. Chem.* **1993**, *32*, 3088–3092. (c) Arm, K. J.; Williams, J. A. G. *Chem. Commun.* **2005**, 230–232. (d) Lowry, M. S.; Bernhard, S. *Chem.—Eur. J.* **2006**, *12*, 7970–7977.
- (7) Ohsawa, Y.; Sprouse, S.; King, K. A.; Dearmond, M. K.; Hanck, K. W.; Watts, R. J. *J. Phys. Chem.* **1987**, *91*, 1047–1054.
- (8) (a) Lepeltier, M.; Lee, T. K.-M.; Lo, K. W.; Toupet, L.; Le Bozec, H.; Guerchais, V. *Eur. J. Inorg. Chem.* **2005**, 110–117. (b) Araya, J. C.; Gajardo, J.; Moya, S. A.; Aguirre, P.; Toupet, L.; Williams, J. A. G.; Escadeillas, M.; Le Bozec, H.; Guerchais, V. *New J. Chem.* **2010**, *34*, 21–24.
- (9) Dragonetti, C.; Falciola, L.; Mussini, P.; Righetto, S.; Roberto, D.; Ugo, R.; Valore, A.; De Angelis, F.; Fantacci, S.; Sgamellotti, A.; Ramon, M.; Muccini, M. *Inorg. Chem.* **2007**, *46*, 8533–8547.
- (10) (a) Dupau, P.; Renouard, T.; Le Bozec, H. *Tetrahedron. Lett.* **1996**, *37*, 7503–7506. (b) Hilton, A.; Renouard, T.; Maury, O.; Le

- Bozec, H.; Ledoux, I.; Zyss, J. *Chem. Commun.* **1999**, 2521–2522.
- (c) Maury, O.; Guégan, J.-P.; Renouard, T.; Hilton, A.; Dupau, P.; Sandon, N.; Toupet, L.; Le Bozec, H. *New J. Chem.* **2001**, 25, 1553–1566.
- (d) Viau, L.; Maury, O.; Le Bozec, H. *Tetrahedron Lett.* **2004**, 45, 125–128.
- (11) (a) Le Boudier, T.; Maury, O.; Le Bozec, H.; Ledoux, I.; Zyss, J. *Chem. Commun.* **2001**, 2430–2431. (b) Sénéchal, K.; Maury, O.; Le Bozec, H.; Ledoux, I.; Zyss, J. *J. Am. Chem. Soc.* **2002**, 124, 4561–4562. (c) Le Boudier, T.; Maury, O.; Le Bozec, H.; Bondon, A.; Costuas, K.; Amouyal, E.; Zyss, J.; Ledoux, I. *J. Am. Chem. Soc.* **2003**, 125, 12884–12899. (d) Maury, O.; Viau, L.; Sénéchal, K.; Corre, B.; Guégan, J.-P.; Renouard, T.; Ledoux, I.; Zyss, J.; Le Bozec, H. *Chem.—Eur. J.* **2004**, 10, 4454–4466. (e) Maury, O.; Le Bozec, H. *Acc. Chem. Res.* **2005**, 38, 691–704. (f) Baccouche, A.; Peigné, B.; Ibersiene, F.; Hammoutène, D.; Boutarfaïa, A.; Boucekkine, A.; Feuvrie, C.; Maury, O.; Ledoux, I.; Le Bozec, H. *J. Phys. Chem. A* **2010**, 114, 5429–5438.
- (12) (a) Dragonetti, C.; Righetto, S.; Roberto, D.; Ugo, R.; Valore, A.; Fantacci, S.; Sgamellotti, A.; De Angelis, F. *Chem. Commun.* **2007**, 4116–4118. (b) Valore, A.; Cariati, E.; Dragonetti, C.; Righetto, S.; Roberto, D.; Ugo, R.; De Angelis, F.; Fantacci, S.; Sgamellotti, A.; Macchioni, A.; Zuccaccia, D. *Chem.—Eur. J.* **2010**, 16, 4814–4825.
- (13) (a) Aubert, V.; Guerchais, V.; Ishow, E.; Hoang-Thi, K.; Ledoux, I.; Nakatani, K.; Le Bozec, H. *Angew. Chem., Int. Ed.* **2008**, 47, 577–580. (b) Aubert, V.; Ishow, E.; Guerchais, V.; Le Bozec, H.; Ibersiene, F.; Boucekkine, A.; Toupet, L.; Métivier, R.; Williams, J. A. G. *New J. Chem.* **2009**, 33, 1320–1323.
- (14) Irie, M. *Chem. Rev.* **2000**, 100, 1685–1716.
- (15) Guerchais, V.; Ordroneau, L.; Le Bozec, H. *Coord. Chem. Rev.* **2010**, 254, 2533–2545 and references cited.
- (16) (a) Lepeltier, M.; Lee, T. K.-M.; Lo, K. K.-W.; Le Bozec, H.; Guerchais, V. *Organometallics* **2005**, 25, 6069–6072. (b) Lepeltier, M.; Lee, T. K.-M.; Lo, K. K.-W.; Le Bozec, H.; Guerchais, V. *Eur. J. Inorg. Chem.* **2007**, 2734–2747.
- (17) (a) Flamigni, L.; Barbieri, A.; Sabatini, C.; Ventura, B.; Barigelletti, F. *Top. Curr. Chem.* **2007**, 281, 143–203. (b) Williams, J. A. G.; Wilkinson, A. J.; Whittle, V. L. *Dalton Trans.* **2008**, 2081–2099.
- (18) For examples of X-ray crystal structures, see inter alia: (a) Neve, F.; Crispini, A. *Eur. J. Inorg. Chem.* **2000**, 1039–1043. (b) Lo, K. K.; Chan, J. S.; Chung, C.; Tsang, V. W.; Zhu, N. *Inorg. Chim. Acta* **2004**, 357, 3109–3118. (c) Neve, F.; La Deda, M.; Crispini, A.; Belluci, A.; Punterio, F.; Campagna, S. *Organometallics* **2004**, 23, 5856–5863. (d) Li, J.; Djurovich, P. I.; Alleyne, B. D.; Yousufuddin, M.; Ho, N. N.; Thomas, J. C.; Peters, J. C.; Bau, R.; Thompson, M. E. *Inorg. Chem.* **2005**, 44, 1713–1727. (e) Zao, N.; Wu, Y.-H.; Wen, H.-M.; Zhang, X.; Chen, Z.-N. *Organometallics* **2009**, 28, 5603–5611.
- (19) Yin, B.; Niemeyer, F.; Williams, J. A. G.; Jiang, J.; Boucekkine, A.; Toupet, L.; Le Bozec, H.; Guerchais, V. *Inorg. Chem.* **2006**, 45, 8584–8596.
- (20) The EFISH technique can be used for the determination of the $\mu\beta$ values of ionic species by operating in a solvent of low polarity and by using a very short duration ($<1 \mu\text{s}$) poling electric field synchronized with laser pulses; as a consequence, ions pairs are not fully dissociated, as shown experimentally by the invariance of the poling field measured between the electrodes of the EFISH cell when replacing the pure solvent by a solution of ionic species. Alain, V.; Blanchard-Desce, M.; Ledoux-Rak, I.; Zyss, J. *Chem. Commun.* **2000**, 353–354.
- (21) For reviews on the application of PGSE NMR to the investigation of intermolecular interactions: (a) Binotti, B.; Macchioni, A.; Zuccaccia, C.; Zuccaccia, D. *Comments Inorg. Chem.* **2002**, 23, 417–450. (b) Pregosin, P. S.; Martinez-Viviente, E.; Kumar, P. G. A. *Dalton Trans.* **2003**, 4007–4014. (c) Bagno, A.; Rastrelli, F.; Saielli, G. *Prog. Nucl. Magn. Reson. Spectrosc.* **2005**, 47, 41–93. (d) Brand, T.; Cabrita, E. J.; Berger, S. *Prog. Nucl. Magn. Reson. Spectrosc.* **2005**, 46, 159–196. (e) Cohen, Y.; Avram, L.; Frish, L. *Angew. Chem., Int. Ed.* **2005**, 44, 520–554. (f) Pregosin, P. S.; Kumar, P. G. A.; Fernández, I. *Chem. Rev.* **2005**, 105, 2977–2998. (f) Pregosin, P. S. *Prog. Nucl. Magn. Reson. Spectrosc.* **2006**, 49, 261–288.
- (22) Guggenheim, E. A. *Trans. Faraday Soc.* **1949**, 45, 714–720.
- (23) Deuterated DMF is particularly suitable for HLS measurements due to its better transparency with respect to DMF. Campo, J.; Wenseleers, W.; Goovaerts, E.; Szablewski, M.; Cross, G. H. *J. Phys. Chem. C* **2008**, 112, 287–296.
- (24) Valore, A.; Cariati, E.; Righetto, S.; Roberto, D.; Tessore, F.; Ugo, R.; Fragalà, I. L.; Fragalà, M. E.; Malandrino, G.; De Angelis, F.; Belpassi, L.; Ledoux-Rak, I.; Thi, K. H.; Zyss, J. *J. Am. Chem. Soc.* **2010**, 132, 4966–4970.
- (25) (a) Brasselet, S.; Zyss, J. *J. Opt. Soc. Am. B* **1998**, 15, 257–288. (b) Zyss, J. *J. Chem. Phys.* **1993**, 98, 6583–6599. (c) Brasselet, S. Ph.D. Thesis; Université de Paris XI Orsay: France, 1997.
- (26) (a) Lee, I.; You, Y.; Lim, S.-J.; Park, S. Y. *Chem. Lett.* **2007**, 36, 888–889. (b) Tan, W.; Zhang, Q.; Zhang, J.; Tian, H. *Org. Lett.* **2009**, 11, 161–164.
- (27) (a) Adamo, C.; Barone, V. *J. Chem. Phys.* **1999**, 110, 6158–6170. (b) Ernzerhof, M.; Scuseria, G. E. *J. Chem. Phys.* **1999**, 110, 5029–5036.
- (28) Frisch, M. J.; Trucks, G. W.; Schlegel, H. B.; Scuseria, G. E.; Robb, M. A.; Cheeseman, J. R.; Montgomery, J. A.; Vreven, T.; Kudin, Jr. K. N.; Burant, J. C.; Millam, J. M.; Iyengar, S. S.; Tomasi, J.; Barone, V.; Mennucci, B.; Cossi, M.; Scalmani, G.; Rega, N.; Petersson, G. A.; Nakatsuji, H.; Hada, M.; Ehara, M.; Toyota, K.; Fukuda, R.; Hasegawa, J.; Ishida, M.; Nakajima, T.; Honda, Y.; Kitao, O.; Nakai, H.; Klene, M.; Li, X.; Knox, J. E.; Hratchian, H. P.; Cross, J. B.; Bakken, V.; Adamo, C.; Jaramillo, J.; Gomperts, R.; Stratmann, R. E.; Yazyev, O.; Austin, A. J.; Cammi, R.; Pomelli, C.; Ochterski, J. W.; Ayala, P. Y.; Morokuma, K.; Voth, G. A.; Salvador, P.; Dannenberg, J. J.; Zakrzewski, V. G.; Dapprich, S.; Daniels, A. D.; Strain, M. C.; Farkas, O.; Malick, D. K.; Rabuck, A. D.; Raghavachari, K.; Foresman, J. B.; Ortiz, J. V.; Cui, Q.; Baboul, A. G.; Clifford, S.; Cioslowski, J.; Stefanov, B. B.; Liu, G.; Liashenko, A.; Piskorz, P.; Komaromi, I.; Martin, R. L.; Fox, D. J.; Keith, T.; Al-Laham, M. A.; Peng, C. Y.; Nanayakkara, A.; Challacombe, M.; Gill, P. M. W.; Johnson, B.; Chen, W.; Wong, M. W.; Gonzalez, C.; Pople, J. A. *Gaussian 03*, revision C.02; Gaussian, Inc.: Wallingford, CT, 2004.
- (29) Flükiger, P.; Lüthi, H. P.; Portmann, S.; Weber, J. *Molekel 4.3*; Swiss Center for Scientific Computing: Manno, Switzerland, 2000; <http://www.cscs.ch/molkel/>.
- (30) (a) Goreslsky, S. I. *SWizard program*, revision 4.5; University of Ottawa: Ottawa, Canada; <http://www.sg-chem.net/swizard>. (b) Goreslsky, S. I.; Lever, A. B. P. *J. Organomet. Chem.* **2001**, 635, 187–196.
- (31) Ledoux, I.; Zyss, J. *Chem. Phys.* **1982**, 73, 203–213.
- (32) (a) Maker, P. D. *Phys. Rev. A* **1970**, 1, 923–951. (b) Clays, K.; Persoons, A. *Phys. Rev. Lett.* **1991**, 66, 2980–2983. (c) Zyss, J.; Ledoux, I. *Chem. Rev.* **1994**, 94, 77–105.